JOURNAL OF GUIDANCE, CONTROL, AND DYNAMICS
Vol. 32, No. 2, March–April 2009

Application of Synchronization to Formation Flying Spacecraft: Lagrangian Approach

Soon-Jo Chung*
Iowa State University, Ames, Iowa 50011
and
Umair Ahsun† and Jean-Jacques E. Slotine‡
Massachusetts Institute of Technology, Cambridge, Massachusetts 02139

DOI: 10.2514/1.37261

This paper presents a unified synchronization framework with application to precision formation flying spacecraft. Central to the proposed innovation, in applying synchronization to both translational and rotational dynamics in the Lagrangian form, is the use of the distributed stability and performance analysis tool, called contraction analysis that yields exact nonlinear stability proofs. The proposed decentralized tracking control law synchronizes the attitude of an arbitrary number of spacecraft into a common time-varying trajectory with global exponential convergence. Moreover, a decentralized translational tracking control law based on oscillator phase synchronization is presented, thus enabling coupled translational and rotational maneuvers. Although the translational dynamics can be adequately controlled by linear control laws, the proposed method permits highly nonlinear systems with nonlinearly coupled inertia matrices such as the attitude dynamics of spacecraft whose large and rapid slew maneuvers justify the nonlinear control approach. The proposed method integrates both the trajectory tracking and synchronization problems in a single control framework.

I. Introduction

MOTIVATED by distributed computation and cooperation, abundant in both biological systems (e.g., fish swarms) and artificial machines (e.g., parallel computers), formation flying spacecraft has been a key research topic among many recent advancements [1–4]. Multiple apertures flying in precise formation are expected to provide unprecedented image resolution, both for astronomy and reconnaissance [5], as well as unparalleled reconfigurability. However, many significant technical challenges must be overcome before formation flying interferometers can be realized (see two representative missions in Fig. 1). For instance, formation flight requires extensive technology development for precise attitude and position maintenance of multiple spacecraft.

The objective of this paper is to introduce a unified synchronization framework that can be directly applied to the position and attitude synchronization, and cooperative control of formation flight networks, composed of either identical or heterogenous spacecraft. Synchronization is defined as a complete match of all configuration variables of each dynamical system. We also introduce phase synchronization where spacecraft follow an oscillatory trajectory with some phase difference between spacecraft. In particular, we show that we can synchronize the attitudes and positions of multiple spacecraft faster than they track the common position and attitude trajectories. The combined synchronization and tracking control law can achieve more efficient and robust performance through local interactions, especially in the presence of nonidentical disturbances and uncertainties. Such local interactions are key to stellar formation flight interferometers that depend on precision control of relative spacecraft motions, indispensable for a coherent interferometric beam combination (see Fig. 1).

A recent review paper [6,7] highlighted the three main areas for future research that have not been thoroughly addressed in the spacecraft formation flight literature: 1) rigorous stability conditions for cyclic and behavioral architectures, 2) reduced algorithmic information requirements, and 3) increased robustness/autonomy. Although this paper does not provide complete solutions to these three challenges, we compare this paper with prior work in the aforementioned areas as follows:

1) Rigorous Stability Condition for Highly Nonlinear Time-Varying Systems. Prior work on consensus and flocking problems using graphs, particularly popular in the robotics research community, tends to assume very simple dynamics such as linear systems and single or double integrator dynamic models [8–11]. Such work can be generally applied to the synchronous spacecraft position control problem, which fares well with linear control. In contrast, the proposed strategy in this paper primarily deals with complex dynamical networks consisting of highly nonlinear time-varying dynamics that are controlled to track a time-varying reference trajectory or leader. Examples of such a nonlinear system include the attitude dynamics of spacecraft for large and rapid slew maneuvers.

Some prior works on attitude synchronization rely on tracking a common reference (leader) spacecraft or nearest neighbor without local information flows [12–14]. Local coupling control laws are suggested in [15], but individual spacecraft are synchronized to a constant state, thus not permitting an arbitrary reference trajectory. This is particularly true of consensus problems on graphs [8]. In [16], a new coordination architecture for both attitude and translational dynamics was proposed to incorporate leader–following, behavioral, and virtual-structure approaches. A decentralized control law using the virtual-structure approach was presented for a potentially large number of spacecraft in [17]. Decentralized attitude control laws with global asymptotic convergence were introduced in [18]. Compared with one recent work [19,20] that studied formation keeping and attitude alignment for multiple spacecraft with local couplings, the present paper introduces both the new attitude synchronization strategy with global exponential convergence and the novel position consensus strategy using phase synchronization.

Presented as Paper 6861 at the AIAA Guidance, Navigation, and Control Conference and Exhibit, Hilton Head, South Carolina, 20–23 August 2007; received 22 February 2008; revision received 24 September 2008; accepted for publication 24 September 2008.

*Assistant Professor of Aerospace Engineering; sjchung@alum.mit.edu. Senior Member AIAA.

†Research Affiliate, MIT Space Systems Laboratory; umair@alum.mit.edu.

‡Professor of Mechanical Engineering and Information Sciences, Professor of Brain and Cognitive Sciences; jjs@mit.edu.

a) NASA formation flying interferometer terrestrial planet finder (TPF) (courtesy: NASA, http://planetquest.jpl.nasa.gov. [1]).

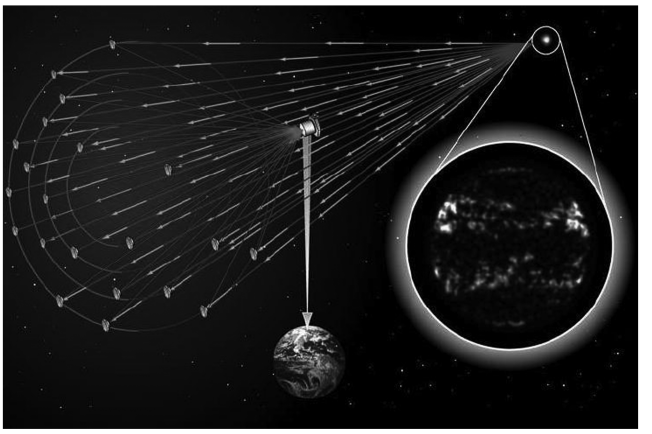

b) NASA Stellar Imager (SI) (courtesy: NASA, http://hires.gsfc.nasa.gov/si. [1]).

Fig. 1 Representative future NASA missions using formation flying spacecraft.

Previously, phase synchronization of a simple planar phase model of fish was studied in [21].

It should be noted that determining stability of nonlinear time-varying dynamic network systems is more involved and difficult [22–24]. Many mechanical systems exhibit nonlinear dynamics that cannot be captured by linearization. One might argue that most space systems are not required to follow demanding time-varying trajectories, thus validating linearization or linear coupling control laws. In particular, for the translational dynamics, a linear coupling control law can effectively stabilize the formation flying spacecraft. However, global exponential convergence of the attitude dynamics is achieved only through nonlinear control. For instance, there is increased interest in highly agile imaging spacecraft [25] that undergo wide and rapid slew angle changes. Moreover, in the context of nonlinear control theory, the asymptotic convergence of linear control, employed to stabilize nonlinear systems, may not be sufficient for demanding future mission requirements. In essence, ensuring exponential tracking stability for general nonlinear systems is made possible only through nonlinear control, and the benefit of exponential stability, in terms of improved tracking performance and robustness, is illustrated in this paper.

We introduce contraction analysis [26–29] as our main nonlinear stability tool for reducing the complexity and dimensionality associated with multi-agent systems, thereby deriving exact and global results with exponential convergence with respect to arbitrary time-varying inputs (see the Appendix for the further treatment of contraction theory).

2) Reduced Information Network. Another benefit of synchronization is its implication for model reduction. The exponential synchronization of multiple nonlinear dynamics allows us to reduce the dimensionality of the stability analysis of a large network. The model reduction aspect of synchronization, also introduced for spatially interconnected systems in [2], is further generalized and strengthened in this paper. This implies that once the network is proven to synchronize, we can regard a network as a single set of synchronized dynamics, which simplifies any additional stability analysis. As shall be seen later in the subsequent sections, this model reduction has to do with the fact that there are two time scales associated with the coupled nonlinear dynamics.

In addition, the proposed control laws are of a decentralized form requiring only local velocity/position coupling feedback for global exponential convergence, thereby facilitating implementation in real systems. In contrast with some previous work using all-to-all coupling or depending only on tracking the same leader (reference) spacecraft without local interactions [13,14], our proposed approach will not only reduce communication burdens, but also increase the overall performance of relative formation flight through local interactions. Further, we mathematically prove that the synchronized maneuvers can also be achieved by sharing partial-state information. This partial degrees-of-freedom coupling will further reduce the amount of formation state information needed for formation flight. Another recent work using the passive decomposition [30] described a strategy of decoupling into the same system representing the internal group formation shape and the locked system describing the total group maneuver.

3) Robustness Issues. The proposed method in this paper integrates both the trajectory tracking and synchronization problems toward a single control framework. Although an uncoupled trajectory control law, in the absence of external disturbances, would achieve synchronization to a common trajectory, the proposed control strategy can achieve more efficient and robust performance through synchronization using local interactions, especially if the external disturbances vary with each spacecraft [22]. In addition, most previous works do not discuss a property of robustness in detail. In contrast, we show that the proposed decentralized control law possesses a property of robustness to interspacecraft time delays and bounded disturbances. An adaptive version of the proposed control law is also presented to deal with parametric uncertainties of dynamic models.

4) Control of Relative Translational Motions. Whereas the present paper presents the unified decentralized control method for the Lagrangian dynamics of both rotational and translational motions of the spacecraft, with focus on minimizing the tracking and synchronization errors, the literature focused only on the relative translational motions is abundant. A decentralized formation control law is presented in [31]. A disturbance accommodating the control design process is presented in [32] for minimizing the total fuel consumption for the formation as well as maintaining the equal level of fuel consumption for each spacecraft. Kasdin et al. [33] present a Hamiltonian approach to modeling relative spacecraft motion based on a derivation of canonical coordinates for the relative state-space dynamics. A formation control law based on Gauss's variational equations was first introduced in [34], while a recent paper [35] presented a new linear time-varying form of the equations of relative motions developed from Gauss's variational equations. A sliding mode controller for Hill's relative motion equations was presented in [36]. This paper presents a synchronization control law for the nonlinear relative spacecraft dynamics, although the proposed approach can be applied to any Lagrangian formulation of spacecraft motions including Hill's equations.

Compared with our recent paper [22] that first reported the combined synchronization and tracking control law for multiple robots, this paper presents the Lagrangian formulation of spacecraft dynamics (Sec. II), introduces a new strategy for oscillator phase synchronization that enables coupled rotational and translational maneuvers (Sec. IV), and discusses the properties of robustness to transmission delays and disturbances more thoroughly (Sec. V). A few examples of formation flying spacecraft are given in Sec. VI for validating the effectiveness of the proposed synchronization framework.

II. Lagrangian Formulation of Formation Flying Spacecraft

The proposed synchronization framework is devoted to the use of the Lagrangian formulation for its simplicity in dealing with complex systems involving multiple dynamics. We show herein that the rotational maneuvers of a rigid spacecraft can be written in this Lagrangian form, thereby permitting direct application of the proposed synchronization strategy [4,22] to the rotational dynamics of multiple spacecraft. Without loss of generality, the proposed control law can be applied to the position synchronization of formation flying spacecraft, or more generally to the coupled translational and attitude dynamics.

A. Lagrangian Formulation

The equations of motion for a spacecraft with multiple degrees of freedom ($\mathbf{q}_i \in \mathbb{R}^n$) can be derived by exploiting the Euler–Lagrange equations:

$$\begin{aligned} L_i(\mathbf{q}_i, \dot{\mathbf{q}}_i) &= \frac{1}{2}\dot{\mathbf{q}}_i^T \mathbf{M}_i(\mathbf{q}_i)\dot{\mathbf{q}}_i - V_i(\mathbf{q}_i) \\ \frac{d}{dt}\frac{\partial L_i(\mathbf{q}_i, \dot{\mathbf{q}}_i)}{\partial \dot{\mathbf{q}}_i} &- \frac{\partial L_i(\mathbf{q}_i, \dot{\mathbf{q}}_i)}{\partial \mathbf{q}_i} = \tau_i \end{aligned} \tag{1}$$

where i ($1 \le i \le p$) denotes the index of spacecraft comprising a spacecraft formation flight network, and p is the total number of the individual elements. Equation (1) can be written as

$$\mathbf{M}_i(\mathbf{q}_i)\ddot{\mathbf{q}}_i + \mathbf{C}_i(\mathbf{q}_i, \dot{\mathbf{q}}_i)\dot{\mathbf{q}}_i + \mathbf{g}_i(\mathbf{q}_i) = \tau_i \tag{2}$$

where

$$\mathbf{g}_i(\mathbf{q}_i) = \frac{dV_i(\mathbf{q}_i)}{d\mathbf{q}_i}$$

and t is a generalized force or torque acting on the ith spacecraft.

It should be emphasized that, among many possible choices, the $\mathbf{C}$ matrix is defined as

$$c_{ij} = \frac{1}{2}\sum_{k=1}^{n}\frac{\partial M_{ij}}{\partial q_k}\dot{q}_k + \frac{1}{2}\sum_{k=1}^{n}\left(\frac{\partial M_{ik}}{\partial q_j} - \frac{\partial M_{jk}}{\partial q_i}\right)\dot{q}_k \tag{3}$$

Then, it is straightforward to show that $(\dot{\mathbf{M}}_i - 2\mathbf{C}_i)$ is skew symmetric, resulting in

$$\mathbf{x}^T(\dot{\mathbf{M}}_i - 2\mathbf{C}_i)\mathbf{x} = 0, \qquad 1 \le i \le p \tag{4}$$

for an arbitrary $\mathbf{x} \in \mathbb{R}^n$. This skew-symmetric property can be viewed as a matrix expression of energy conservation, which can also be explained in the context of the passivity formalism [23]. In the remainder of this paper, the property in Eq. (4) is extensively exploited for stability analysis and control synthesis using contraction theory [4].

We assume that the spacecraft system in Eq. (2) is fully actuated. In other words, the number of control inputs is equal to the dimension of their configuration manifold (n). However, we do not require the communication of the full state information for the purpose of synchronization, as shall be seen in Sec. VI.A.

B. Attitude Dynamics of Rigid Spacecraft

The aim of this section is to show that we can establish a Lagrangian formulation given in Eq. (2) from the rotational attitude dynamics of a rigid spacecraft ($n = 3$). We improve the approach in [37] in two aspects. First, we introduce the generalized form to explore the increasing interest in agile imaging spacecraft using a control moment gyroscope (CMG) [25] and a variable speed control moment gyroscope (VSCMG) [38]. Second, we incorporate the modified Rodrigues parameters (MRPs) [39,40], in lieu of the Rodrigues parameters, to overcome the singularity problem at the rotation of ± 180 deg.

Using the Euler rotational equations of motion, the following equation describes the angular velocity vector $\omega \in \mathbb{R}^3$ of the spacecraft in its body axes:

$$\mathbf{J}_{s/c}\dot{\omega} - (\mathbf{J}_{s/c}\omega) \times \omega = \mathbf{u} + \mathbf{d}_{ext} \tag{5}$$

where the internal control torque $\mathbf{u}$, generated either by VSCMGs or CMGs, is defined as [25]

$$\mathbf{u} = -\dot{\mathbf{h}} + \mathbf{h} \times \omega \tag{6}$$

Based on Eq. (6), a suitable algorithm, such as the pseudoinverse steering logic [25], can determine the gimbal angle vector g once the control input $\mathbf{u}$ is computed from the attitude control law.

Note that the matrix $\mathbf{J}_{s/c}$ is the total moment of inertia of the spacecraft, expressed in its body frame, and is symmetric positive definite. Also, $\mathbf{h}$ and $\mathbf{d}_{ext}$, all expressed in the spacecraft body-fixed frame, denote the total control momentum vector by CMGs, and the external disturbance torque such as the aerodynamic drag torque and the gravity gradient torque. We also assume that the change of $\mathbf{J}_{s/c}$ due to the CMG gimbal angular rate is small (i.e., $\dot{\mathbf{J}}_{s/c} = 0$).

In the case of VSCMGs, the control momentum vector ($\mathbf{h}$) and its rate ($\dot{\mathbf{h}}$) can be written as [38]

$$\begin{aligned} \mathbf{h} &= \mathbf{A}_g\mathbf{I}_g\dot{\gamma} + \mathbf{A}_s\mathbf{I}_w\boldsymbol{\Omega} \\ \dot{\mathbf{h}} &= \mathbf{A}_g\mathbf{I}_g\ddot{\gamma} + \mathbf{A}_s\mathbf{I}_w\dot{\boldsymbol{\Omega}} + \mathbf{A}_t\mathbf{I}_w\mathrm{diag}(\dot{\boldsymbol{\Omega}})\dot{\gamma} \end{aligned} \tag{7}$$

where g and $\boldsymbol{\Omega}$ denote the gimbal angles and wheel speeds of the VSCMGs, respectively, while $\mathbf{I}_g$ and $\mathbf{I}_w$ are the moment of inertia of the gimbal structure and the wheel. Also, $\mathbf{A}_g$, $\mathbf{A}_s$, and $\mathbf{A}_t$ denote the transformation matrices associated with the body-frame representation [38].

The purpose of introducing Eq. (7) is to show that Eq. (5) may represent either the rotational dynamics of spacecraft with fixed-speed CMGs (constant $\boldsymbol{\Omega}$) or reaction wheels ($\dot{\gamma} = 0$).

To avoid the singularity problem of the Euler angular representation, it is often preferred to use quaternions to represent an angular orientation between two different coordinate frames:

$$\begin{aligned} \beta_1 &= e_1 \sin\frac{\theta}{2}, \qquad \beta_2 = e_2 \sin\frac{\theta}{2} \\ \beta_3 &= e_3 \sin\frac{\theta}{2}, \qquad \beta_4 = \cos\frac{\theta}{2} \end{aligned} \tag{8}$$

where $\mathbf{e} = (e_1, e_2, e_3)^T$ is the Euler axis of rotation expressed in the body frame and θ is the rotation angle about $\mathbf{e}$.

The modified Rodrigues parameters can be written as [39,40]

$$\mathbf{q} = (q_1, q_2, q_3)^T = \mathbf{e}\tan\frac{\theta}{4} \tag{9}$$

Then, the attitude of the spacecraft has the following relation:

$$\dot{\mathbf{q}} = \mathbf{Z}(\mathbf{q})\omega \tag{10}$$

where

$$\begin{aligned} \mathbf{Z}(\mathbf{q}) &= \frac{1}{2}\left[\mathbf{I}\left(\frac{1-\mathbf{q}^T\mathbf{q}}{2}\right) + \mathbf{q}\mathbf{q}^T + \mathbf{S}(\mathbf{q})\right] \\ &= \frac{1}{4}\begin{bmatrix} (1+q_1^2-q_2^2-q_3^2) & 2(q_1q_2-q_3) & 2(q_1q_3+q_2) \\ 2(q_2q_1+q_3) & (1-q_1^2+q_2^2-q_3^2) & 2(q_2q_3-q_1) \\ 2(q_3q_1-q_2) & 2(q_3q_2+q_1) & (1-q_1^2-q_2^2+q_3^2) \end{bmatrix} \end{aligned} \tag{11}$$

and the skew-symmetric matrix function, $\mathbf{S}(\mathbf{x})$ for an arbitrary $\mathbf{x} \in \mathbb{R}^3$ is defined as

$$\mathbf{S}(\mathbf{x}) = \begin{bmatrix} 0 & -x_3 & x_2 \\ x_3 & 0 & -x_1 \\ -x_2 & x_1 & 0 \end{bmatrix} \tag{12}$$

Also, note that the corresponding quaternions in Eq. (8) can be obtained from the modified Rodrigues parameters by the following transformation:

$$\begin{aligned}\beta_i &= 2q_i/(1+\mathbf{q}^T\mathbf{q}), \qquad i=1,2,3\\ \beta_4 &= (1-\mathbf{q}^T\mathbf{q})/(1+\mathbf{q}^T\mathbf{q})\end{aligned} \tag{13}$$

while its inverse transformation can be written

$$q_i = \beta_i/(1+\beta_4), \qquad i=1,2,3 \tag{14}$$

By combining Eqs. (5) and (10), the following equations of motion are obtained with respect to the modified Rodrigues parameters $\mathbf{q}_i$ for the ith spacecraft ($1 \le i \le p$)

$$\mathbf{M}_i(\mathbf{q}_i)\ddot{\mathbf{q}}_i + \mathbf{C}_i(\mathbf{q}_i,\dot{\mathbf{q}}_i)\dot{\mathbf{q}}_i = \tau_i + \tau_{\text{ext},i} \tag{15}$$

where

$$\begin{aligned}\tau_i &= \mathbf{Z}^{-T}(\mathbf{q}_i)\mathbf{u}, \qquad \tau_{\text{ext},i} = \mathbf{Z}^{-T}(\mathbf{q}_i)\mathbf{d}_{\text{ext},i}\\ \mathbf{M}_i(\mathbf{q}_i) &= \mathbf{Z}^{-T}(\mathbf{q}_i)\mathbf{J}_{\text{s/c},i}\mathbf{Z}^{-1}(\mathbf{q}_i)\\ \mathbf{C}_i(\mathbf{q}_i,\dot{\mathbf{q}}_i) &= -\mathbf{Z}^{-T}\mathbf{J}_{\text{s/c},i}\mathbf{Z}^{-1}\dot{\mathbf{Z}}\mathbf{Z}^{-1} - \mathbf{Z}^{-T}\mathbf{S}(\mathbf{J}_{\text{s/c},i}\omega_i)\mathbf{Z}^{-1}\end{aligned} \tag{16}$$

Notice that the index i has been added to $\mathbf{J}_{\text{s/c},i}$ (hence, also to $\mathbf{M}_i$ and $\mathbf{C}_i$) to permit complex formation networks composed of multiple heterogeneous spacecraft. Also, note that

$$\mathbf{S}(\mathbf{J}_{\text{s/c},i}\omega_i) = \mathbf{S}(\mathbf{J}_{\text{s/c},i}\mathbf{Z}^{-1}(\mathbf{q}_i)\dot{\mathbf{q}}_i)$$

from Eq. (10). Notice that all the terms in Eqs. (15) and (16) are left multiplied by $\mathbf{Z}^{-T}(\mathbf{q}_i)$. However, we should not cancel out the common term $\mathbf{Z}^{-T}(\mathbf{q}_i)$ of Eqs. (15) and (16), which would result in having a nonsymmetric $\mathbf{M}_i(\mathbf{q}_i)$. In essence, we established a Lagrangian formulation for the attitude dynamics of rigid spacecraft. This allows us to apply a wealth of nonlinear control laws to spacecraft dynamics, including the proposed control strategy in [22], that were originally developed for robot dynamics. As discussed in Eq. (4), the most important feature of Eq. (15) is to have a skew-symmetric $\dot{\mathbf{M}} - 2\mathbf{C}$ due to energy conservation. Indeed, we can verify that

$$\begin{aligned}\dot{\mathbf{M}}_i - 2\mathbf{C}_i &= \frac{\mathrm{d}\mathbf{Z}^{-T}}{\mathrm{d}t}\mathbf{J}_{\text{s/c},i}\mathbf{Z}^{-1} - \mathbf{Z}^{-T}\mathbf{J}_{\text{s/c},i}\frac{\mathrm{d}\mathbf{Z}^{-1}}{\mathrm{d}t}\\ &\quad + 2\mathbf{Z}^{-T}\mathbf{S}(\mathbf{J}_{\text{s/c},i}\omega_i)\mathbf{Z}^{-1}\end{aligned} \tag{17}$$

is skew symmetric, which follows that $\mathbf{S}(\mathbf{J}_{\text{s/c},i}\omega_i)$ is skew symmetric. Without loss of generality, the control torque $\mathbf{u}$ generated by momentum wheels ($\dot{\gamma} = 0$) can be defined as $\mathbf{u}_i = -\dot{\mathbf{h}}_i$. Then, the $\mathbf{S}(\mathbf{J}_{\text{s/c},i}\omega_i)$ in Eq. (16) is replaced by $\mathbf{S}(\mathbf{J}_{\text{s/c},i}\omega_i + \mathbf{h}_i)$ to account for the gyro stiffening effect of the wheels.

In the subsequent sections, the rotational dynamics formulation in Eq. (15) is used to develop a nonlinear synchronization tracking control law for multiple formation flying spacecraft.

C. Relative Translational Dynamics

If we assume that the influence of the attitude dynamics on the translational dynamics is weak and ignored, the translational dynamics, modeled as double integrators [6], can be easily augmented with the attitude dynamics in Eq. (15). Alternatively, similar to [14,41], the coupled translational and rotational motions of formation spacecraft can be written in the Lagrangian form in Eq. (2). Then, the proposed decentralized tracking control can be effectively applied without loss of generality. For arbitrary translational dynamics, synchronization corresponds to $\mathbf{x}_1 = \mathbf{x}_2 = \cdots = \mathbf{x}_p$ where $\mathbf{x}_i$, $1 \le i \le p$ connotes a vector of biased variables constructed from the position vector $\mathbf{r}_i$ such that $\mathbf{r}_i(t) = \mathbf{x}_i(t) + \mathbf{b}_i(t)$ and the separation vector $\mathbf{b}_i(t)$ is independent of the dynamics [4]. Conceptually, such a method follows that each position vector $\mathbf{x}_i$ can be defined from virtually shifted origins. In this paper, the goal is to take a different approach in which the phase differences of the position variables can synchronize on a spiral or circular trajectory.

In pursuit of this goal, this section presents relative translational dynamics applicable to formation flight on a circular or spiral configuration in low Earth orbit such that the formation translational control is based on the relative dynamics with respect to the desired formation center of mass (c.m.). For deriving a relative position control law, it is more advantageous to work in the noninertial orbital coordinates F^{RO} as illustrated in Fig. 2. The orbital frame F^{RO} is defined in such a way that its origin is attached to the center of mass of the formation with its y axis aligned with the position vector $\mathbf{R}_0$ representing the position of the formation center of mass in the Earth centered inertial frame. The z axis points toward the orbital plane normal and the x axis completes the right-hand system (see Fig. 2).

Although this derivation can also be done in an orbital frame attached to the *leader* satellite, the leader satellite will be maneuvering in general so its orbital velocity would not be a constant. Therefore, it is more accurate to use an orbital reference frame attached to the center of mass of the formation as opposed to the leader satellite.

For simplicity, we will assume a circular reference orbit for the formation center of mass for which the angular velocity of the reference orbit is simply

$$\omega_0 = \sqrt{\frac{\mu_e}{R_0^3}} \tag{18}$$

where μ_e is the gravitational constant of Earth ($398,600.4418 \times 10^9\ \mathrm{m}^3/\mathrm{s}^2$) and R_0 is the radius of the formation's center of mass orbit.

Even though we consider the J_2 effects as a source of disturbance for simulation studies in this paper, we ignore the J_2 terms for the control law development. Then, the relative dynamics of the ith satellite with respect to satellite k in the orbital frame F^{RO} can be written as [3]

$$\begin{aligned}&\ddot{x}_i - 2\omega_0\dot{y}_i - \omega_0^2 x_i + \frac{\mu_e x_i}{R_i^3} = \frac{F_x + F_{xd}}{m}\\ &\ddot{y}_i + 2\omega_0\dot{x}_i - \omega_0^2 y_i + \frac{\mu_e(R_0+y_i)}{R_i^3} - \frac{\mu_e}{R_0^2} = \frac{F_y + F_{yd}}{m}\\ &\ddot{z}_i + \frac{\mu_e z_i}{R_i^3} = \frac{F_z + F_{zd}}{m}\end{aligned} \tag{19}$$

where F_x, F_y, and F_z denote the control forces while F_{xd}, F_{yd}, and F_{zd} represent the external disturbance forces, all expressed in the orbital frame F^{RO}. In addition, the distance between the Earth's center and the ith satellite is defined as

$$R_i = \sqrt{x_i^2 + (y_i + R_0)^2 + z_i^2} \tag{20}$$

Ignoring the disturbances, Eq. (19) can be written in a Lagrangian form with a constant mass matrix, similar to Eq. (2)

$$\mathbf{M}\ddot{\mathbf{r}}_i + \mathbf{C}\dot{\mathbf{r}}_i + \mathbf{D}(\mathbf{r}_i)\mathbf{r}_i + \mathbf{g}(\mathbf{r}_i) = \mathbf{F}_i \tag{21}$$

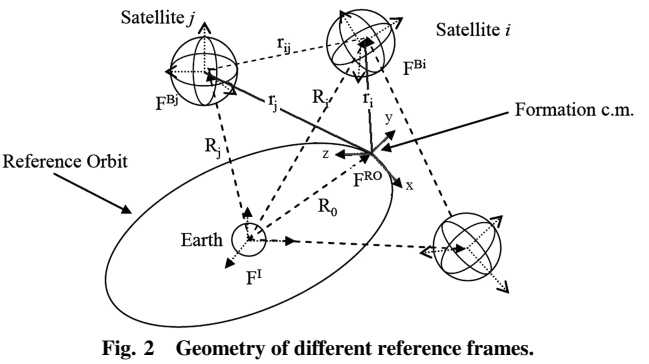

Fig. 2 Geometry of different reference frames.

where

$$\mathbf{M} = \begin{bmatrix} m & 0 & 0 \\ 0 & m & 0 \\ 0 & 0 & m \end{bmatrix}, \qquad \mathbf{r}_i = \begin{pmatrix} x_i \\ y_i \\ z_i \end{pmatrix}$$
$$\mathbf{C} = \begin{bmatrix} 0 & -2m\omega_0 & 0 \\ 2m\omega_0 & 0 & 0 \\ 0 & 0 & 0 \end{bmatrix}, \qquad \mathbf{F}_i = \begin{pmatrix} F_x \\ F_y \\ F_z \end{pmatrix} \tag{22}$$
$$\mathbf{D}(\mathbf{r}_i) = \begin{bmatrix} -m\omega_0^2 + m\frac{\mu_e}{R_i^3} & 0 & 0 \\ 0 & -m\omega_0^2 + m\frac{\mu_e}{R_i^3} & 0 \\ 0 & 0 & \frac{\mu_e}{R_i^3} \end{bmatrix}$$
$$\mathbf{g}(\mathbf{r}_i) = \begin{pmatrix} 0 \\ m\left(\frac{\mu_e R_0}{R_i^3} - \frac{\mu_e}{R_0^2}\right) \\ 0 \end{pmatrix}$$

We make two important remarks regarding Eq. (21). First, as opposed to the attitude dynamics of spacecraft in the preceding section, $\mathbf{M}$ and $\mathbf{C}$ are constant, which simplifies the stability proofs. Nonetheless, $\dot{\mathbf{M}} - 2\mathbf{C}$ is skew symmetric, which unifies our control law design for both attitude and translational dynamics. Note that the $\mathbf{C}$ matrix in Eq. (21) is not obtained from Eq. (3). Second, if the difference between R_i and R_0 is reasonably small, $\mathbf{D}(\mathbf{r}_i)$ becomes a constant matrix such that $\mathbf{D} = \mathrm{diag}(0, 0, \omega_0^2)$. This may further simplify the proposed control law in Sec. IV.

III. Decentralized Nonlinear Control for Attitude Synchronization

We consider the attitude synchronization of multiple spacecraft following a common time-varying trajectory in this section.

A. Attitude Synchronization of Spacecraft

The following decentralized tracking control law with two-way-ring symmetry is proposed for the ith spacecraft in the network composed of p spacecraft (see Figs. 3a and 3b):

$$\tau_i = \mathbf{M}_i(\mathbf{q}_i)\ddot{\mathbf{q}}_{r,i} + \mathbf{C}_i(\mathbf{q}_i, \dot{\mathbf{q}}_i)\dot{\mathbf{q}}_{r,i} + \mathbf{g}_i(\mathbf{q}_i) - \mathbf{K}_1\mathbf{s}_i + \mathbf{K}_2\mathbf{s}_{i-1} + \mathbf{K}_2\mathbf{s}_{i+1} \tag{23}$$

where a positive-definite matrix $\mathbf{K}_1 \in \mathbb{R}^{n\times n}$ is a feedback gain for the ith satellite, and another positive-definite matrix $\mathbf{K}_2 \in \mathbb{R}^{n\times n}$ is a coupling gain with the adjacent members ($i-1$ and $i+1$). For two-spacecraft networks, the last coupling term with the $i+1$th member in Eq. (23) is not used. It should be emphasized that the assumption of the bidirectional coupling in Eq. (23) can be relaxed without loss of generality to account for a regular digraph [22]. Also, $\dot{\mathbf{q}}_{r,i}$ and $\mathbf{s}_i$ are defined such that

$$\begin{aligned} \dot{\mathbf{q}}_{r,i} &= \dot{\mathbf{q}}_d(t) + \mathbf{\Lambda}(\mathbf{q}_d(t) - \mathbf{q}_i) \\ \mathbf{s}_i &= \dot{\mathbf{q}}_i - \dot{\mathbf{q}}_{r,i} = \dot{\mathbf{q}}_i - \dot{\mathbf{q}}_d(t) + \mathbf{\Lambda}(\mathbf{q}_i - \mathbf{q}_d(t)) \end{aligned} \tag{24}$$

where $\mathbf{\Lambda}$ is a positive diagonal matrix. The time-varying desired trajectory $\mathbf{q}_d(t)$ can be the formation flying guidance command or the trajectory of a leader spacecraft.

If we assume that a relative attitude metrology system, similar to [42,43], is available in addition to each spacecraft's own attitude measurement with respect to the inertial frame, the relative attitude errors (e.g., $\mathbf{q}_{i+1} - \mathbf{q}_i$) can be computed. In turn, nonlinear observers can estimate the velocity errors (e.g., $\dot{\mathbf{q}}_{i+1} - \dot{\mathbf{q}}_i$), we can rewrite Eq. (23) as

$$\begin{aligned} \tau_i = \mathbf{M}_i(\mathbf{q}_i)\ddot{\mathbf{q}}_{r,i} + \mathbf{C}_i(\mathbf{q}_i, \dot{\mathbf{q}}_i)\dot{\mathbf{q}}_{r,i} + \mathbf{g}_i(\mathbf{q}_i) - (\mathbf{K}_1 - 2\mathbf{K}_2)\mathbf{s}_i \\ + \mathbf{K}_2[(\dot{\mathbf{q}}_{i-1} - \dot{\mathbf{q}}_i) + \mathbf{\Lambda}(\mathbf{q}_{i-1} - \mathbf{q}_i)] + \mathbf{K}_2[(\dot{\mathbf{q}}_{i+1} - \dot{\mathbf{q}}_i) \\ + \mathbf{\Lambda}(\mathbf{q}_{i+1} - \mathbf{q}_i)] \end{aligned} \tag{25}$$

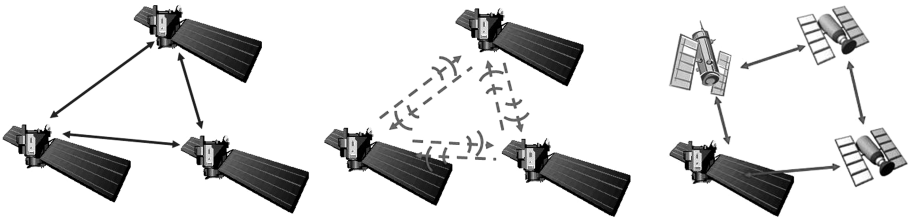

a) Network of identical spacecraft via communication coupling (left) or relative sensing (right)

b) Nonidentical spacecraft

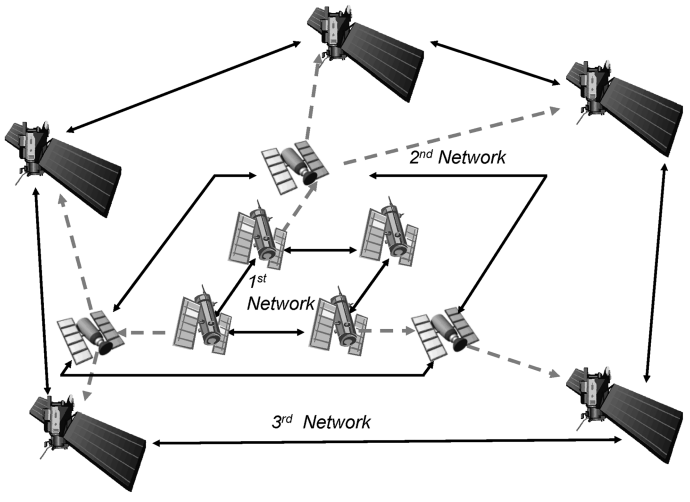

c) Concurrent synchronization of multiple spacecraft groups

Fig. 3 Formation flying networks of a) identical or b) nonidentical spacecraft using local couplings considered in this paper. They are on balanced bidirectional regular graphs, but a more complex geometry or leader–follower network can also be constructed by concurrent synchronization c) [22]. Also, without loss of generality, the bidirectional couplings can be extended to unidirectional couplings [22].

This can be straightforwardly applied to the translational dynamics with relative distance measurements [44], as shall be seen in Sec. IV. This implies that such a relative sensing system can eliminate the need for exchanging the state information of each spacecraft; no intersatellite communication would be required. In essence, we can implement the proposed decentralized control law by either the communication links or the relative metrology system, as illustrated in Fig. 3.

It should be noted again that one of the main contributions of this paper lies with the use of a new differential stability framework, yielding the exact proof of nonlinear stability under a variety of conditions. Note that the above control law requires only the coupling feedback of the most adjacent spacecraft ($i-1$ and $i+1$) for exponential convergence (see Fig. 3). Consequently, the last (pth) satellite is connected with the first satellite to form a ring network as suggested in [28]. To construct a more complex geometry rather than a single ring network (e.g., see Fig. 3c), concurrent synchronization [45] can be used as expanded upon in [4,22].

Without loss of generality, we can extend the proposed control law to adaptive control [23]

$$\tau_i = \mathbf{Y}_i\hat{\mathbf{a}}_i - \mathbf{K}_1\mathbf{s}_i + \mathbf{K}_2\mathbf{s}_{i-1} + \mathbf{K}_2\mathbf{s}_{i+1} = \hat{\mathbf{M}}_i\ddot{\mathbf{q}}_{r,i} + \hat{\mathbf{C}}_i\dot{\mathbf{q}}_{r,i} + \hat{\mathbf{g}}_i(\mathbf{q}_i) - \mathbf{K}_1\mathbf{s}_i + \mathbf{K}_2\mathbf{s}_{i-1} + \mathbf{K}_2\mathbf{s}_{i+1} \tag{26}$$

The parameter estimate $\hat{\mathbf{a}}_i$ for the ith member is updated by the correlation integral:

$$\dot{\hat{\mathbf{a}}}_i = -\Gamma\mathbf{Y}_i^T\mathbf{s}_i \tag{27}$$

where Γ is a symmetric positive-definite matrix. The stability proof of the adaptive control law, presented in [22], does not alter the main proofs in this paper except that the convergence result reduces to asymptotic instead of exponential. Hence, we will only focus on the general control law in Eq. (2) for the sake of simplicity.

The closed-loop dynamics for the whole formation, by using Eqs. (2) and (23), can be written as

$$[\mathbf{M}]\dot{\mathbf{x}} + [\mathbf{C}]\mathbf{x} + [\mathbf{L}^p_{\mathbf{K}_1,-\mathbf{K}_2}]\mathbf{x} = \mathbf{0} \tag{28}$$

where

$$[\mathbf{M}] = \begin{bmatrix} \mathbf{M}_1(\mathbf{q}_1) & \cdots & \mathbf{0} \\ \vdots & \ddots & \vdots \\ \mathbf{0} & \cdots & \mathbf{M}_p(\mathbf{q}_p) \end{bmatrix}$$

$$[\mathbf{C}] = \begin{bmatrix} \mathbf{C}_1(\mathbf{q}_1,\dot{\mathbf{q}}_1) & \cdots & \mathbf{0} \\ \vdots & \ddots & \vdots \\ \mathbf{0} & \cdots & \mathbf{C}_p(\mathbf{q}_p,\dot{\mathbf{q}}_p) \end{bmatrix}, \qquad \mathbf{x} = \begin{pmatrix} \mathbf{s}_1 \\ \vdots \\ \mathbf{s}_p \end{pmatrix} \tag{29}$$

Also, the $pn \times pn$ block matrix $[\mathbf{L}^p_{\mathbf{K}_1,-\mathbf{K}_2}]$ has $\mathbf{K}_1$ as its diagonal matrix elements, neighbored by $-\mathbf{K}_2$. In other words, from the definition of the controller in Eq. (23), $[\mathbf{L}^p_{\mathbf{K}_1,-\mathbf{K}_2}]$ has only three nonzero matrix elements in each row (i.e., $\mathbf{K}_1$, $\mathbf{K}_2$, and $\mathbf{K}_2$).

The network graphs illustrated in Fig. 3 are *balanced* due to bidirectional coupling [8]. However, it should be noted that the matrix $[\mathbf{L}^p_{\mathbf{K}_1,-\mathbf{K}_2}]$ is different from the standard weighted Laplacian found in [8]. By definition, every row sum of the Laplacian matrix on a balanced graph is zero. Hence, the Laplacian matrix always has a zero eigenvalue corresponding to a right eigenvector, $\mathbf{1} = (1,1,\ldots,1)^T$ [8]. In contrast, a strictly positive-definite $[\mathbf{L}^p_{\mathbf{K}_1,-\mathbf{K}_2}]$ is required for exponential convergence for the proposed control law in this paper.

We present the main theorems of the paper. First, the following condition should be true for exponential convergence to a common desired trajectory $\mathbf{q}_d(t)$.

Theorem III.1: Global Exponential Convergence to the Desired Trajectory. If $[\mathbf{L}^p_{\mathbf{K}_1,-\mathbf{K}_2}]$ is uniformly positive definite, then every member of the network follows the desired trajectory $\mathbf{q}_d(t)$ exponentially fast regardless of initial conditions. In other words, if $\mathbf{K}_1 - 2\mathbf{K}_2 > 0$, then $\mathbf{q}_i$, $(i = 1,2,\ldots,p,\ p \geq 3)$ converges to $\mathbf{q}_d(t)$ exponentially fast from any initial conditions. For two-spacecraft systems ($p = 2$), $\mathbf{K}_1 - \mathbf{K}_2 > 0$ needs to be true instead.

Proof: We present a new proof that emphasizes the hierarchical combination structure of the proposed control law. Equation (28) of the closed-loop dynamics corresponds to a conventional tracking problem.

Recalling Theorem VII.2, we construct the following hierarchical virtual system of $\mathbf{y}_1$ and $\mathbf{y}_2$:

$$\begin{bmatrix} [\mathbf{M}] & \mathbf{0} \\ \mathbf{0} & \mathbf{I} \end{bmatrix}\begin{pmatrix} \dot{\mathbf{y}}_1 \\ \dot{\mathbf{y}}_2 \end{pmatrix} + \begin{bmatrix} [\mathbf{C}] + [\mathbf{L}^p_{\mathbf{K}_1,-\mathbf{K}_2}] & \mathbf{0} \\ -\mathbf{I} & [\mathbf{\Lambda}] \end{bmatrix}\begin{pmatrix} \mathbf{y}_1 \\ \mathbf{y}_2 \end{pmatrix} = \begin{pmatrix} \mathbf{0} \\ \mathbf{0} \end{pmatrix} \tag{30}$$

where the virtual system of $\mathbf{y}_1$ is obtained by replacing $\mathbf{x}$ with $\mathbf{y}_1$ in Eq. (28), and the system of $\mathbf{y}_2$ is from the definition of the composite variable in Eq. (24). Also, $[\mathbf{\Lambda}] = \mathrm{diag}(\mathbf{\Lambda},\ldots,\mathbf{\Lambda})$.

It is straightforward to verify that Eq. (30) has two particular solutions:

$$\begin{pmatrix} \mathbf{y}_1 = \mathbf{x} \\ \mathbf{y}_2 = \{\tilde{\mathbf{q}}\} \end{pmatrix} \quad \text{and} \quad \begin{pmatrix} \mathbf{y}_1 = \mathbf{0} \\ \mathbf{y}_2 = \mathbf{0} \end{pmatrix}, \quad \text{where } \{\tilde{\mathbf{q}}\} = \begin{pmatrix} \mathbf{q}_1 - \mathbf{q}_d \\ \vdots \\ \mathbf{q}_p - \mathbf{q}_d \end{pmatrix} \tag{31}$$

The differential virtual length analysis with respect to the uniformly positive-definite metric,

$$\begin{bmatrix} [\mathbf{M}] & \mathbf{0} \\ \mathbf{0} & \alpha\mathbf{I} \end{bmatrix}, \qquad \exists\alpha > 0 \tag{32}$$

yields

$$\begin{aligned} \frac{d}{\mathrm{d}t}\begin{pmatrix} \delta\mathbf{y}_1 \\ \delta\mathbf{y}_2 \end{pmatrix}^T\begin{bmatrix} [\mathbf{M}] & \mathbf{0} \\ \mathbf{0} & \alpha\mathbf{I} \end{bmatrix}\begin{pmatrix} \delta\mathbf{y}_1 \\ \delta\mathbf{y}_2 \end{pmatrix} &= \begin{pmatrix} \delta\mathbf{y}_1 \\ \delta\mathbf{y}_2 \end{pmatrix}^T\begin{bmatrix} [\dot{\mathbf{M}}] & \mathbf{0} \\ \mathbf{0} & \mathbf{0} \end{bmatrix}\begin{pmatrix} \delta\mathbf{y}_1 \\ \delta\mathbf{y}_2 \end{pmatrix} \\ &\quad + 2\begin{pmatrix} \delta\mathbf{y}_1 \\ \delta\mathbf{y}_2 \end{pmatrix}^T\begin{bmatrix} [\mathbf{M}] & \mathbf{0} \\ \mathbf{0} & \alpha\mathbf{I} \end{bmatrix}\begin{pmatrix} \delta\dot{\mathbf{y}}_1 \\ \delta\dot{\mathbf{y}}_2 \end{pmatrix} \\ &= \begin{pmatrix} \delta\mathbf{y}_1 \\ \delta\mathbf{y}_2 \end{pmatrix}^T\begin{bmatrix} [\dot{\mathbf{M}}] & \mathbf{0} \\ \mathbf{0} & \mathbf{0} \end{bmatrix}\begin{pmatrix} \delta\mathbf{y}_1 \\ \delta\mathbf{y}_2 \end{pmatrix} \\ &\quad + 2\begin{pmatrix} \delta\mathbf{y}_1 \\ \delta\mathbf{y}_2 \end{pmatrix}^T\begin{bmatrix} -[\mathbf{C}] - [\mathbf{L}^p_{\mathbf{K}_1,-\mathbf{K}_2}] & \mathbf{0} \\ \alpha\mathbf{I} & -\alpha[\mathbf{\Lambda}] \end{bmatrix}\begin{pmatrix} \delta\mathbf{y}_1 \\ \delta\mathbf{y}_2 \end{pmatrix} \\ &= \begin{pmatrix} \delta\mathbf{y}_1 \\ \delta\mathbf{y}_2 \end{pmatrix}^T\begin{bmatrix} -2[\mathbf{L}^p_{\mathbf{K}_1,-\mathbf{K}_2}] & \mathbf{0} \\ 2\alpha\mathbf{I} & -2\alpha[\mathbf{\Lambda}] \end{bmatrix}\begin{pmatrix} \delta\mathbf{y}_1 \\ \delta\mathbf{y}_2 \end{pmatrix} \\ &= \begin{pmatrix} \delta\mathbf{y}_1 \\ \delta\mathbf{y}_2 \end{pmatrix}^T\mathbf{B}\begin{pmatrix} \delta\mathbf{y}_1 \\ \delta\mathbf{y}_2 \end{pmatrix} \end{aligned} \tag{33}$$

where we used the skew-symmetric property of $[\dot{\mathbf{M}}] - 2[\mathbf{C}]$.

The symmetric part of the matrix $\mathbf{B}$ is

$$\mathbf{B}_s = \frac{1}{2}(\mathbf{B} + \mathbf{B}^T) = \begin{bmatrix} -2[\mathbf{L}^p_{\mathbf{K}_1,-\mathbf{K}_2}] & \alpha\mathbf{I} \\ \alpha\mathbf{I} & -2\alpha[\mathbf{\Lambda}] \end{bmatrix} \tag{34}$$

According to Theorem VII.1, Eq. (30) is contracting if the symmetric matrix $\mathbf{B}_s$ is uniformly negative definite. We can always find $\alpha > 0$ such that $\mathbf{B}_s$ is uniformly negative definite:

$$\alpha\mathbf{I} < 4[\mathbf{L}^p_{\mathbf{K}_1,-\mathbf{K}_2}][\mathbf{\Lambda}], \qquad [\mathbf{L}^p_{\mathbf{K}_1,-\mathbf{K}_2}] > 0, \quad \text{and} \quad \mathbf{\Lambda} > 0 \tag{35}$$

Accordingly, all solutions of Eq. (30) converge to each other exponentially fast, resulting in global exponential convergence of $\mathbf{q}$ to $\mathbf{q}_d(t)$. The positive definiteness of $[\mathbf{L}^p_{\mathbf{K}_1,-\mathbf{K}_2}]$ corresponds to $\mathbf{K}_1 - \mathbf{K}_2 > 0$ for two-spacecraft systems ($p = 2$). For a network consisting of more than two spacecraft ($p \geq 3$), it can be shown that $\mathbf{K}_1 - 2\mathbf{K}_2$

is a sufficient condition of the positive definiteness of $[\mathbf{L}^p_{\mathbf{K}_1,-\mathbf{K}_2}]$ given $\mathbf{K}_1 > 0$, $\mathbf{K}_2 > 0$.

We now focus on the synchronization of multiple spacecraft dynamics. First, we introduce an orthogonal matrix, whose column vectors constitute a superset of the flow-invariant subspace of synchronization [22,45] such that $\mathbf{V}^T_{\text{sync}}\mathbf{x} = 0$.

Since $[\mathbf{L}^p_{\mathbf{K}_1,-\mathbf{K}_2}]$ is a constant real symmetric matrix, we can perform the spectral decomposition

$$[\mathbf{L}^p_{\mathbf{K}_1,-\mathbf{K}_2}] = \mathbf{V}[\mathbf{D}]\mathbf{V}^T, \qquad [\mathbf{D}] = \mathbf{V}^T[\mathbf{L}^p_{\mathbf{K}_1,-\mathbf{K}_2}]\mathbf{V} \tag{36}$$

where $[\mathbf{D}]$ is a block diagonal matrix, and the square matrix $\mathbf{V}$ is composed of the orthonormal eigenvectors. Because the symmetry of $[\mathbf{L}^p_{\mathbf{K}_1,-\mathbf{K}_2}]$ gives rise to real eigenvalues and orthonormal eigenvectors [46], we can verify that $\mathbf{V}^T\mathbf{V} = \mathbf{V}\mathbf{V}^T = \mathbf{I}_{pn}$.

The modified Laplacian $[\mathbf{L}^p_{\mathbf{K}_1,-\mathbf{K}_2}]$ defines a *regular* graph, where each member has the same number of neighbors (=2 for $p \geq 3$). A regular graph has the block column identify matrix $[\mathbf{1}] = [\mathbf{I}_n, \mathbf{I}_n, \ldots, \mathbf{I}_n]^T/\sqrt{p}$ as its eigenvectors associated with the tracking convergence rate $\lambda(\mathbf{K}_1 - 2\mathbf{K}_2)$ for $p \geq 3$. Hence, we can define a $pn \times (p-1)n$ matrix $\mathbf{V}_{\text{sync}}$ constructed from the orthonormal eigenvectors other than $[\mathbf{1}]$ such that

$$\mathbf{V}^T\mathbf{V} = \begin{pmatrix} [\mathbf{1}]^T \\ \mathbf{V}^T_{\text{sync}} \end{pmatrix}([\mathbf{1}] \quad \mathbf{V}_{\text{sync}}) = \begin{bmatrix} [\mathbf{1}]^T[\mathbf{1}] & [\mathbf{1}]^T\mathbf{V}_{\text{sync}} \\ \mathbf{V}^T_{\text{sync}}[\mathbf{1}] & \mathbf{V}^T_{\text{sync}}\mathbf{V}_{\text{sync}} \end{bmatrix} = \begin{bmatrix} \mathbf{I}_n & \mathbf{0}_{n\times(p-1)n} \\ \mathbf{0}_{(p-1)n\times n} & \mathbf{I}_{(p-1)n} \end{bmatrix} \tag{37}$$

where we used the orthogonality between $[\mathbf{1}]$ and $\mathbf{V}_{\text{sync}}$.

The synchronization of multiple spacecraft $\mathbf{q}_1 = \mathbf{q}_2 = \cdots = \mathbf{q}_p$ corresponds to

$$\mathbf{V}^T_{\text{sync}}\begin{pmatrix} \mathbf{q}_1 \\ \vdots \\ \mathbf{q}_p \end{pmatrix} = \mathbf{0} \tag{38}$$

Theorem III.2: Synchronization of Multiple Identical or Heterogeneous Spacecraft [22]. A network of p spacecraft synchronizes exponentially from any initial conditions if $\exists$ diagonal matrices $\mathbf{K}_1 > 0$, $\mathbf{K}_2 > 0$ such that

$$\mathbf{V}^T_{\text{sync}}[\mathbf{L}^p_{\mathbf{K}_1,-\mathbf{K}_2}]\mathbf{V}_{\text{sync}} > 0$$

In addition, $\mathbf{\Lambda}$ is a positive diagonal matrix defining a stable composite variable $\mathbf{s}_i = \dot{\tilde{\mathbf{q}}}_i + \mathbf{\Lambda}\tilde{\mathbf{q}}_i$ with $\tilde{\mathbf{q}}_i = \mathbf{q}_i - \mathbf{q}_d(t)$.

If we have unidirectional couplings on a regular graph, the preceding conditions are replaced by $\mathbf{V}^T_{\text{sync}}([\mathbf{L}^p_{\mathbf{K}_1,-\mathbf{K}_2}] + [\mathbf{L}^p_{\mathbf{K}_1,-\mathbf{K}_2}]^T)\mathbf{V}_{\text{sync}} > 0$ (see [22] for details). This Theorem corresponds to synchronization with stable tracking. Multiple dynamics need not be identical to achieve stable synchronization. It should be noted that Theorem III.2 can be used, regardless of Theorem III.1. For example, $[\mathbf{L}^p_{\mathbf{K}_1,-\mathbf{K}_2}]$ might be semipositive definite, thus yielding indifferent tracking dynamics. In this case, we do not need a common reference trajectory for the synchronization of multiple spacecraft, and the spacecraft synchronize to the average of the initial conditions (see [22] for details). It is useful to note that the above condition corresponds to $\mathbf{K}_1 + \mathbf{K}_2 > 0$ for two-spacecraft and three-spacecraft networks ($p = 2, 3$).

Note that we can make the system synchronize first, then follow the common trajectory by tuning the gains properly. This indicates that there exist two different time scales in the closed-loop systems constructed with the proposed controllers. For two-spacecraft systems, the convergence of exponential tracking is proportional to $\mathbf{K}_1 - \mathbf{K}_2$, whereas the synchronization has a convergence rate of $\mathbf{K}_1 + \mathbf{K}_2$. This multitime-scale behavior will be exploited in the subsequent sections.

B. Proof of Exponential Synchronization

We summarize the proof of Theorem III.2 for the exponential synchronization of multiple nonlinear dynamics, first reported in [22]. The key result can be generalized for an arbitrary number of spacecraft, even to more complex structures beyond a standard ring geometry [22].

Suppose that $\mathbf{M}(\mathbf{q})$ is a constant inertia matrix $\mathbf{M}$, thereby resulting in $\mathbf{C}(\mathbf{q}, \dot{\mathbf{q}}) = \mathbf{0}$. Then, we can easily prove $\mathbf{s}_1$ and $\mathbf{s}_2$ tend to each other using Theorem VII.4. On the other hand, the difficulties associated with nonlinear time-varying inertia matrices can be easily demonstrated. In essence, $\mathbf{M}(\mathbf{q}_1) \neq \mathbf{M}(\mathbf{q}_2)$ makes this problem intractable in general. We now present a solution to this open problem, focused on the synchronization of multiple spacecraft with nonconstant nonlinear metrics.

Recall the closed-loop dynamics given in Eq. (28). Premultiplying Eq. (28) by $\mathbf{V}^T$ and setting $\mathbf{x} = \mathbf{V}\mathbf{V}^T\mathbf{x}$ results in

$$(\mathbf{V}^T[\mathbf{M}]\mathbf{V})\dot{\mathbf{z}} + (\mathbf{V}^T[\mathbf{C}]\mathbf{V})\mathbf{z} + [\mathbf{D}]\mathbf{z} = \mathbf{0} \tag{39}$$

where $\mathbf{z} = \mathbf{V}^T\mathbf{x}$.

Then, we can develop the squared-length analysis similar to Eq. (33). Notice that $(\mathbf{V}^T[\mathbf{M}]\mathbf{V})$ is always symmetric positive definite since $[\mathbf{M}]$ is symmetric positive definite.

Using Eq. (37), the block diagonal matrix $[\mathbf{D}]$, which represents the eigenvalues of $[\mathbf{L}^p_{\mathbf{K}_1,-\mathbf{K}_2}]$, can be partitioned from Eq. (36)

$$\mathbf{V}^T[\mathbf{L}^p_{\mathbf{K}_1,-\mathbf{K}_2}]\mathbf{V} = \begin{bmatrix} [\mathbf{1}]^T[\mathbf{L}^p_{\mathbf{K}_1,-\mathbf{K}_2}][\mathbf{1}] & [\mathbf{1}]^T[\mathbf{L}^p_{\mathbf{K}_1,-\mathbf{K}_2}]\mathbf{V}_{\text{sync}} \\ \mathbf{V}^T_{\text{sync}}[\mathbf{L}^p_{\mathbf{K}_1,-\mathbf{K}_2}][\mathbf{1}] & \mathbf{V}^T_{\text{sync}}[\mathbf{L}^p_{\mathbf{K}_1,-\mathbf{K}_2}]\mathbf{V}_{\text{sync}} \end{bmatrix} = \begin{bmatrix} \mathbf{D}_1 & \mathbf{0}_{n\times(p-1)n} \\ \mathbf{0}_{(p-1)n\times n} & \mathbf{D}_2 \end{bmatrix} \tag{40}$$

It should be noted that $\mathbf{D}_1 = \mathbf{K}_1 - 2\mathbf{K}_2$ for $p \geq 3$ (or $\mathbf{D}_1 = \mathbf{K}_1 - \mathbf{K}_2$ for $p = 2$) represents the tracking gain while $\mathbf{D}_2$ corresponds to the synchronization gain. We can choose the control gain matrices $\mathbf{K}_1$ and $\mathbf{K}_2$ such that

$$\mathbf{D}_2 = \mathbf{V}^T_{\text{sync}}[\mathbf{L}^p_{\mathbf{K}_1,-\mathbf{K}_2}]\mathbf{V}_{\text{sync}} > \mathbf{D}_1 = [\mathbf{1}]^T[\mathbf{L}^p_{\mathbf{K}_1,-\mathbf{K}_2}][\mathbf{1}] \tag{41}$$

This will ensure that multiple spacecraft synchronize faster than they follow the common desired trajectory. In other words, multiple spacecraft synchronize first, then they converge to the desired trajectory while staying together.

Now let us write the virtual system of $\mathbf{y}$ by replacing $\mathbf{z}$ in Eq. (39) with $\mathbf{y}$:

$$(\mathbf{V}^T[\mathbf{M}]\mathbf{V})\dot{\mathbf{y}} + (\mathbf{V}^T[\mathbf{C}]\mathbf{V})\mathbf{y} + [\mathbf{D}]\mathbf{y} = \mathbf{0} \tag{42}$$

The above system has the following particular solutions:

$$\mathbf{y} = \begin{pmatrix} \mathbf{y}_t \\ \mathbf{y}_s \end{pmatrix} = \begin{pmatrix} [\mathbf{1}]^T\mathbf{x} \\ \mathbf{V}^T_{\text{sync}}\mathbf{x} \end{pmatrix} \quad \text{and} \quad \mathbf{y} = \begin{pmatrix} \mathbf{y}_t \\ \mathbf{y}_s \end{pmatrix} = \begin{pmatrix} \mathbf{0} \\ \mathbf{0} \end{pmatrix} \tag{43}$$

Now we need to prove that the system in Eq. (42) is contracting (i.e., $\delta\mathbf{y} \to \mathbf{0}$ globally and exponentially) to show that those two solutions tend exponentially to each other. Performing the squared-length analysis with respect to the symmetric positive-definite block matrix $\mathbf{V}^T[\mathbf{M}]\mathbf{V}$ as the contraction metric yields

$$\frac{\mathrm{d}}{\mathrm{d}t}\begin{pmatrix} \delta\mathbf{y}_t \\ \delta\mathbf{y}_s \end{pmatrix}^T\begin{bmatrix} [\mathbf{1}]^T[\mathbf{M}][\mathbf{1}] & [\mathbf{1}]^T[\mathbf{M}]\mathbf{V}_{\text{sync}} \\ \mathbf{V}^T_{\text{sync}}[\mathbf{M}][\mathbf{1}] & \mathbf{V}^T_{\text{sync}}[\mathbf{M}]\mathbf{V}_{\text{sync}} \end{bmatrix}\begin{pmatrix} \delta\mathbf{y}_t \\ \delta\mathbf{y}_s \end{pmatrix} = -2\begin{pmatrix} \delta\mathbf{y}_t \\ \delta\mathbf{y}_s \end{pmatrix}^T\begin{bmatrix} \mathbf{D}_1 & \mathbf{0} \\ \mathbf{0} & \mathbf{D}_2 \end{bmatrix}\begin{pmatrix} \delta\mathbf{y}_t \\ \delta\mathbf{y}_s \end{pmatrix} \tag{44}$$

where we used the skew-symmetric property of $(\mathbf{V}^T[\dot{\mathbf{M}}]\mathbf{V}) - 2(\mathbf{V}^T[\mathbf{C}]\mathbf{V})$.

If $[\mathbf{D}] > 0$, or equivalently $[\mathbf{L}^p_{\mathbf{K}_1,-\mathbf{K}_2}] > 0$, the combined virtual system in Eq. (42) is contracting. This in turn implies that all solutions of $\mathbf{y}$ tend to a single trajectory. As a result, $[\mathbf{1}]^T\mathbf{x} = (\mathbf{s}_1 + \cdots + \mathbf{s}_p)/\sqrt{p}$ and $\mathbf{V}^T_{\text{sync}}\mathbf{x}$ tend exponentially to zero. Note that $\mathbf{s}_1, \ldots, \mathbf{s}_p \to \mathbf{0}$ has already been proven for Theorem III.1. What is

new here is the proof of synchronization $\mathbf{V}_{\text{sync}}^T\mathbf{x} \to \mathbf{0}$. Note that the synchronization occurs even if the tracking dynamics are indifferent ($\mathbf{D}_1 = \mathbf{0}$). Then, $[\mathbf{D}]$ is positive semidefinite, and we can prove the global asymptotic stability of the synchronization $\mathbf{V}_{\text{sync}}^T\mathbf{x} \to \mathbf{0}$ by using Barbalat's lemma (see [22]). This special case agrees with the average consensus problem on graphs.

By exploiting the hierarchical structure (Theorem VII.2) of the composite variable defined in Eq. (24), we can show that $\mathbf{V}_{\text{sync}}^T\mathbf{x} \to \mathbf{0}$ and $\mathbf{\Lambda} > 0$ also make $\mathbf{q}_1, \ldots, \mathbf{q}_p$ synchronize exponentially (i.e., $\mathbf{V}_{\text{sync}}^T(\mathbf{q}_1^T, \ldots, \mathbf{q}_p^T)^T \to \mathbf{0}$). This straightforwardly follows the proof of Theorem III.1.

In the case of identical spacecraft, this synchronization result also implies that the diagonal terms of the metric $\mathbf{V}_{\text{sync}}^T[\mathbf{M}][\mathbf{1}]$ tend to zero exponentially, thereby eliminating the coupling of the inertia term $\mathbf{V}^T[\mathbf{M}]\mathbf{V}$ in Eq. (44). So far, we have assumed that $\mathbf{q}_d(t)$ is identical for each spacecraft. If $\mathbf{q}_d(t)$ were different for each dynamics, $\mathbf{s}_i \to \mathbf{s}_j$ would imply the synchronization of $\mathbf{q}_i - \mathbf{q}_j$ to the difference of the desired trajectories, which would be useful to construct phase synchronization of spacecraft positions. Such phase synchronization is discussed in the subsequent section. It should be mentioned that global asymptotic convergence of a linear coupling control law for the nonlinear attitude dynamics is proven in [22] and compared with the proposed nonlinear control law in Sec. VI.

C. Concurrent Synchronization of a Large Formation

Consider a complex spacecraft network that consists of multiple identical or heterogeneous groups as shown in Figs. 1b and 3c. We exploit the fact that there exist two different time scales of the proposed synchronization tracking control law ($\mathbf{D}_1$ and $\mathbf{D}_2$). In other words, we can exploit a desired reference trajectory $\mathbf{q}_d(t)$ to create multiple combinations of different dynamics groups. For instance, Fig. 3c shows both the diffusive coupling structure proposed by the tracking control law (solid lines) and the reference directional input (dashed lines). Each spacecraft on the same network initially receives a different desired trajectory input from the adjacent spacecraft of the different (inner) network. Once the inner network synchronizes, the outer network also ends up receiving the same desired trajectory to follow, while they interact to synchronize exponentially fast. Accordingly, we can achieve concurrent synchronization [45] between multiple network groups. The proof straightforwardly follows Theorem VII.2. Readers are referred to [22] for further discussions.

IV. Decentralized Nonlinear Control for Relative Translational Dynamics

We introduce a new method for the phase synchronization of multiple spacecraft positions that follow a time-varying circular or spiral trajectory with equal spacing between spacecraft, as shown in Fig. 4. We also illustrate that the rotational and translational dynamics can be combined to enable coupled rotational maneuvers, which can realize a spiral trajectory. The UV coverage of an interferometer defines the size and density of spatial points on the two-dimensional modulation transfer function of an image [4,5]. By spiraling out, a stellar interferometer can construct a virtually large telescope, thereby accomplishing a suitable UV coverage, which in turn results in a finer angular resolution and higher contrast ratio. The kinds of stellar objects that will be observed will also contain information at many spatial frequencies; thus the ability of stellar interferometers to observe at multiple baselines will be key.

A. Rotational Phase Synchronization for Spacecraft Positions

This section extends the phase synchronization of a single variable from [45] to Lagrangian systems of multiple degrees of freedom on a three-dimensional plane with a hierarchical control law. A new proof for phase synchronization is presented such that the angular transformation terms in the Laplacian matrix disappear. By combining the trajectory control with the synchronization coupling, we can achieve much more efficient and robust performance that is essential to precision formation flight of spacecraft.

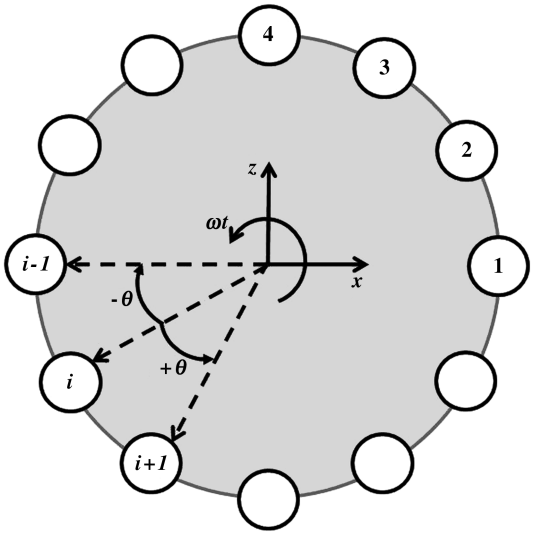

Fig. 4 Geometry of a circular rotating trajectory. The x–z axes denote F^{RO} in Fig. 2.

For the relative translational dynamics presented in Eq. (21), the following decentralized tracking control law with two-way-ring symmetry is proposed for the ith spacecraft in the circular network composed of p *identical* spacecraft ($1 \le i \le p$):

$$\mathbf{F}_i = \mathbf{M}\ddot{\mathbf{r}}_{r,i} + \mathbf{C}\dot{\mathbf{r}}_{r,i} + \mathbf{D}(\mathbf{r}_i)\mathbf{r}_i + \mathbf{g}(\mathbf{r}_i) - k_1\mathbf{s}_i^{\text{pos}} + k_2\mathbf{T}(\theta)\mathbf{s}_{i-1}^{\text{pos}} + k_2\mathbf{T}^T(\theta)\mathbf{s}_{i+1}^{\text{pos}} \tag{45}$$

where k_1 and k_2 are positive constants, and the rotation matrix $\mathbf{T}(\theta) \in \mathcal{SO}(2)$ is defined as

$$\mathbf{T}(\theta) = \begin{bmatrix} \cos\theta & 0 & -\sin\theta \\ 0 & 1 & 0 \\ \sin\theta & 0 & \cos\theta \end{bmatrix} \tag{46}$$

Note that $\mathbf{T}^T(\theta) = \mathbf{T}^{-1}(\theta) = \mathbf{T}(-\theta)$ and $\mathbf{T}(p\theta) = \mathbf{I}$ since $\theta = 2\pi/p$.

For two-spacecraft networks, the last coupling term with the $(i+1)$th member is not used. Also, the shifted reference velocity vector $\dot{\mathbf{r}}_{r,i}$ and the composite variable $\mathbf{s}_i^{\text{pos}}$ are defined as follows:

$$\begin{aligned} \dot{\mathbf{r}}_{r,i} &= \dot{\mathbf{r}}_{d,i} + \lambda(\mathbf{r}_{d,i} - \mathbf{r}_i) \\ \mathbf{s}_i^{\text{pos}} &= \dot{\mathbf{r}}_i - \dot{\mathbf{r}}_{r,i} = \dot{\mathbf{r}}_i - \dot{\mathbf{r}}_{d,i} + \lambda(\mathbf{r}_i - \mathbf{r}_{d,i}) \end{aligned} \tag{47}$$

where λ is a positive constant. The time-varying desired trajectory $\mathbf{r}_{d,i}$ is different for each spacecraft because its phase is shifted from its neighbors by $\pm\theta$:

$$\begin{aligned} &\mathbf{r}_{d,1} = (a(t)\cos\omega t, y_d(t), a(t)\sin\omega t)^T = \mathbf{r}_d \\ &\mathbf{r}_{d,2} = (a(t)\cos[\omega t + \theta], y_d(t), a(t)\sin[\omega t + \theta])^T = \mathbf{T}(\theta)\mathbf{r}_d \\ &\vdots \\ &\mathbf{r}_{d,i} = (a(t)\cos[\omega t + (i-1)\theta], y_d(t), a(t)\sin[\omega t \\ &\quad + (i-1)\theta])^T = \mathbf{T}((i-1)\theta)\mathbf{r}_d \end{aligned} \tag{48}$$

Note that $y_d(t)$ can be a time-varying function, thereby constructing a three-dimensional oscillatory trajectory. In the case of a two-dimensional circular trajectory orthogonal to the orbital plane, the radius $a(t)$ becomes a constant and $y_d(t)$ reduces to zero.

The closed-loop dynamics for the ith satellite, constructed from Eqs. (21) and (45), becomes

$$\mathbf{M}\dot{\mathbf{s}}_i^{\text{pos}} + \mathbf{C}\mathbf{s}_i^{\text{pos}} + k_1\mathbf{s}_i^{\text{pos}} - k_2\mathbf{T}(\theta)\mathbf{s}_{i-1}^{\text{pos}} - k_2\mathbf{T}^T(\theta)\mathbf{s}_{i+1}^{\text{pos}} = \mathbf{0} \tag{49}$$

By inspecting Fig. 4, we can find the new flow-invariant set of $\mathbf{s}_i^{\text{pos}}$ that is phase shifted from the original invariant set

$\mathbf{s}_1^{\text{pos}} = \mathbf{s}_2^{\text{pos}} = \cdots = \mathbf{s}_p^{\text{pos}}$:

$$\mathbf{s}_1^{\text{pos}} = \mathbf{T}^T(\theta)\mathbf{s}_2^{\text{pos}} = \cdots = \mathbf{T}^T((p-1)\theta)\mathbf{s}_p^{\text{pos}} \tag{50}$$

where the matrix of the orthonormal eigenvectors $\mathbf{V}$ is obtained from Eq. (36).

Left multiplying Eq. (49) with $\mathbf{T}^T((i-1)\theta)$ for each spacecraft results in

$$[\mathbf{M}^{\text{pos}}]\ddot{\mathbf{x}}^{\text{pos}} + [\mathbf{C}^{\text{pos}}]\dot{\mathbf{x}}^{\text{pos}} + [\mathbf{L}^p_{\mathbf{K}_1,-\mathbf{K}_2}]\mathbf{x}^{\text{pos}} = \mathbf{0} \tag{51}$$

where

$$[\mathbf{M}^{\text{pos}}] = \begin{bmatrix} \mathbf{M}_{T,1} & \cdots & \mathbf{0} \\ \vdots & \ddots & \vdots \\ \mathbf{0} & \cdots & \mathbf{M}_{T,p} \end{bmatrix}$$

$$[\mathbf{C}^{\text{pos}}] = \begin{bmatrix} \mathbf{C}_{T,1} & \cdots & \mathbf{0} \\ \vdots & \ddots & \vdots \\ \mathbf{0} & \cdots & \mathbf{C}_{T,p} \end{bmatrix}, \qquad \mathbf{x}^{\text{pos}} = \begin{pmatrix} \mathbf{s}_1^{\text{pos}} \\ \vdots \\ \mathbf{T}^T((p-1)\theta)\mathbf{s}_p^{\text{pos}} \end{pmatrix} \tag{52}$$

Also,

$$\mathbf{M}_{T,i} = \mathbf{T}^T((i-1)\theta)\mathbf{M}\mathbf{T}((i-1)\theta) = \mathbf{M}$$

and

$$\mathbf{C}_{T,i} = \mathbf{T}^T((i-1)\theta)\mathbf{C}\mathbf{T}((i-1)\theta)$$

where the $\mathbf{M}$ and $\mathbf{C}$ matrices are defined in Eq. (21). Hence,

$$\dot{\mathbf{M}}_{T,i} - 2\mathbf{C}_{T,i} = -2\mathbf{C}_{T,i}$$

is skew symmetric. Then, similar to the previous section, we can prove the synchronization $\mathbf{V}_{\text{sync}}^T\mathbf{x}^{\text{pos}} \to \mathbf{0}$ as well as the tracking convergence $\mathbf{s}_i^{\text{pos}} \to \mathbf{0}$ by constructing the virtual system and performing the spectral decomposition as follows:

$$(\mathbf{V}^T[\mathbf{M}^{\text{pos}}]\mathbf{V})\ddot{\mathbf{y}} + (\mathbf{V}^T[\mathbf{C}^{\text{pos}}]\mathbf{V})\dot{\mathbf{y}} + [\mathbf{D}]\mathbf{y} = \mathbf{0} \tag{53}$$

Note that Eq. (53) has

$$\mathbf{y} = \mathbf{V}^T\mathbf{x}^{\text{pos}} = ([\mathbf{1}], \mathbf{V}_{\text{sync}})^T\mathbf{x}^{\text{pos}}$$

and $\mathbf{y} = \mathbf{0}$ as particular solutions. Because of the skew symmetry of $\mathbf{C}$, Eq. (53) is contracting with $[\mathbf{D}] > 0$, resulting in the tracking stability $\mathbf{s}_i^{\text{pos}} \to 0$ as well as

$$\mathbf{s}_1^{\text{pos}} \leftrightarrow \mathbf{T}^T(\theta)\mathbf{s}_2^{\text{pos}} \leftrightarrow \mathbf{T}^T((i-1)\theta)\mathbf{s}_i^{\text{pos}} \leftrightarrow \mathbf{T}^T((p-1)\theta)\mathbf{s}_p^{\text{pos}} \tag{54}$$

From the hierarchical combination of the composite variable and the definition of $\mathbf{r}_{d,i}$, one can verify that

$$\begin{aligned} \dot{\mathbf{r}}_i + \lambda\mathbf{r}_i + \mathbf{T}((i-1)\theta)(\dot{\mathbf{r}}_d + \lambda\mathbf{r}_d) &= \mathbf{s}_i^{\text{pos}} \\ \dot{\mathbf{r}}_{i+1} + \lambda\mathbf{r}_{i+1} + \mathbf{T}(i\theta)(\dot{\mathbf{r}}_d + \lambda\mathbf{r}_d) &= \mathbf{s}_{i+1}^{\text{pos}} \end{aligned} \tag{55}$$

Left multiplying the dynamic equation of $\mathbf{r}_i$ in Eq. (55) with $\mathbf{T}^T((i-1)\theta)$, and that of $\mathbf{r}_{i+1}$ with $\mathbf{T}^T((i)\theta)$ results in

$$\begin{aligned} \mathbf{T}^T((i-1)\theta)\dot{\mathbf{r}}_i + \lambda\mathbf{T}^T((i-1)\theta)\mathbf{r}_i &= u(t) \\ \mathbf{T}^T(i\theta)\dot{\mathbf{r}}_{i+1} + \lambda\mathbf{T}^T(i\theta)\mathbf{r}_{i+1} &= u(t) \end{aligned} \tag{56}$$

where the common input verifies $u(t) = -(\dot{\mathbf{r}}_d + \lambda\mathbf{r}_d)$ if the phase-shifted composite variables synchronize, that is,

$$\mathbf{T}^T((i-1)\theta)\mathbf{s}_i^{\text{pos}} = \mathbf{T}^T(i\theta)\mathbf{s}_{i+1}^{\text{pos}}$$

From Eq. (56), $\lambda > 0$ ensures that $\mathbf{T}^T((i-1)\theta)\mathbf{r}_i$ exponentially tends to $\mathbf{T}^T(i\theta)\mathbf{r}_{i+1}$ since $\dot{\mathbf{y}} + \lambda\mathbf{y} = 0$ is contracting (Theorems VII.1 and VII. 4). This concludes the proof of the phase synchronization of the relative translational dynamics for the case of multiple identical spacecraft on a circular or spiral trajectory. For heterogeneous spacecraft, we can scale the control gains k_1 and k_2 according to the mass ratio, and the proof essentially remains the same. Furthermore, we can straightforwardly extend the constant phase shift θ to arbitrarily different phase shifts among spacecraft (i.e., $\theta_i \neq \theta_j$ with $i \neq j$).

B. Synchronized Rotational Maneuvers

One can easily construct the combined dynamics of both attitude rotation and relative position as follows:

$$\begin{bmatrix} [\mathbf{M}] & 0 \\ 0 & [\mathbf{M}^{\text{pos}}] \end{bmatrix}\begin{pmatrix} \ddot{\mathbf{x}} \\ \ddot{\mathbf{x}}^{\text{pos}} \end{pmatrix} + \begin{bmatrix} [\mathbf{C}] & 0 \\ 0 & [\mathbf{C}^{\text{pos}}] \end{bmatrix}\begin{pmatrix} \dot{\mathbf{x}} \\ \dot{\mathbf{x}}^{\text{pos}} \end{pmatrix} + \begin{bmatrix} [\mathbf{L}^p_{\mathbf{K}_1,-\mathbf{K}_2}] & 0 \\ 0 & [\mathbf{L}^p_{\mathbf{K}_1,-\mathbf{K}_2}] \end{bmatrix}\begin{pmatrix} \mathbf{x} \\ \mathbf{x}^{\text{pos}} \end{pmatrix} = \mathbf{0} \tag{57}$$

where we used the control law (23) for the rotational attitude dynamics and the control law (45) for the translational dynamics.

We can also demonstrate the synchronized rotation maneuver [13] by synchronizing the desired rotational rate of the attitude dynamics from $\mathbf{q}_d(t)$ and $\dot{\mathbf{q}}_d(t)$ with the rotational rate ω of the desired circular trajectory $\mathbf{r}_d(t)$ defined in Eq. (48).

V. Effects of Communication Delays and Model Uncertainties

Now let us discuss the robustness properties of the proposed synchronization tracking control approach.

A. Synchronization with Time Delays

Based on [29], we show herein that contraction properties are conserved in time-delayed diffusionlike couplings for multiple Lagrangian dynamics of spacecraft. In particular, the proposed synchronization coupling control law in Eqs. (23) and (45) can be proven to synchronize multiple dynamical systems as well as to track the common trajectory, regardless of time delays in the communication.

Let us consider two spacecraft transmitting their attitude state information to each other via time-delayed transmission channels, as shown in Fig. 5. While T_{12} is a positive constant denoting the time delay in the communication from the first spacecraft to the second spacecraft, T_{21} denotes the delay from the second spacecraft to the first spacecraft.

Similar to [29], we can modify our original Lagrangian systems consisting of two identical spacecraft in Eq. (28) as follows:

$$\begin{aligned} \mathbf{M}(\mathbf{q}_1)\dot{\mathbf{s}}_1 + \mathbf{C}(\mathbf{q}_1, \dot{\mathbf{q}}_1)\mathbf{s}_1 + (\mathbf{K}_1 - \mathbf{K}_2)\mathbf{s}_1 - \mathbf{G}_{21}\tau_{21} &= \mathbf{0} \\ \mathbf{M}(\mathbf{q}_2)\dot{\mathbf{s}}_2 + \mathbf{C}(\mathbf{q}_2, \dot{\mathbf{q}}_2)\mathbf{s}_2 + (\mathbf{K}_1 - \mathbf{K}_2)\mathbf{s}_2 - \mathbf{G}_{12}\tau_{12} &= \mathbf{0} \end{aligned} \tag{58}$$

where $\mathbf{G}_{21}$ and $\mathbf{G}_{12}$ are constant matrices ($\mathbb{R}^{n\times n}$).

The communication between the two dynamics occurs by transmitting intermediate "wave" variables, defined as [29]

$$\begin{aligned} \mathbf{u}_{21} &= \mathbf{G}_{21}^T\mathbf{s}_1 + k_{21}\tau_{21} \qquad & \mathbf{v}_{12} &= \mathbf{G}_{21}^T\mathbf{s}_1 \\ \mathbf{u}_{12} &= \mathbf{G}_{12}^T\mathbf{s}_2 + k_{12}\tau_{12} \qquad & \mathbf{v}_{21} &= \mathbf{G}_{12}^T\mathbf{s}_2 \end{aligned} \tag{59}$$

where k_{21} and k_{12} are strictly positive constants. Time delays of T_{21} and T_{12} result in

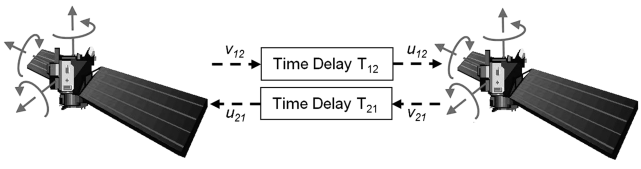

Fig. 5 Synchronization of two identical spacecraft with transmission delays.

$$\mathbf{u}_{12}(t) = \mathbf{v}_{12}(t - T_{12}) \qquad \mathbf{u}_{21}(t) = \mathbf{v}_{21}(t - T_{21}) \tag{60}$$

Notice that the original dynamics without any communication delays are contracting since $\mathbf{K}_1 - \mathbf{K}_2 > 0$. Expanding Eq. (58), using the above relationships on the wave variables, yields

$$\begin{aligned}
&\mathbf{M}(\mathbf{q}_1)\dot{\mathbf{s}}_1 + \mathbf{C}(\mathbf{q}_1, \dot{\mathbf{q}}_1)\mathbf{s}_1 + (\mathbf{K}_1 - \mathbf{K}_2)\mathbf{s}_1 \\
&\quad - \frac{1}{k_{21}}\mathbf{G}_{21}(\mathbf{G}_{12}^T\mathbf{s}_2(t - T_{21}) - \mathbf{G}_{21}^T\mathbf{s}_1(t)) = \mathbf{0} \\
&\mathbf{M}(\mathbf{q}_2)\dot{\mathbf{s}}_2 + \mathbf{C}(\mathbf{q}_2, \dot{\mathbf{q}}_2)\mathbf{s}_2 + (\mathbf{K}_1 - \mathbf{K}_2)\mathbf{s}_2 \\
&\quad - \frac{1}{k_{12}}\mathbf{G}_{12}(\mathbf{G}_{21}^T\mathbf{s}_1(t - T_{12}) - \mathbf{G}_{12}^T\mathbf{s}_2(t)) = \mathbf{0}
\end{aligned} \tag{61}$$

We can verify that Eq. (61) becomes equivalent to the original two-spacecraft dynamics that can be written as in Eq. (28) by setting $k_{12} = k_{21} = 1$ and $\mathbf{G}_{12} = \mathbf{G}_{21} = \sqrt{\mathbf{K}_2}$. Note that $\sqrt{\mathbf{K}_2}$ is the Cholesky decomposition of the positive-definite symmetric matrix, $\mathbf{K}_2$.

The resultant equations reflecting the time-delayed transmissions become

$$\begin{aligned}
&\mathbf{M}(\mathbf{q}_1)\dot{\mathbf{s}}_1 + \mathbf{C}(\mathbf{q}_1, \dot{\mathbf{q}}_1)\mathbf{s}_1 + \mathbf{K}_1\mathbf{s}_1 - \mathbf{K}_2\mathbf{s}_2(t - T_{21}) = \mathbf{0} \\
&\mathbf{M}(\mathbf{q}_2)\dot{\mathbf{s}}_2 + \mathbf{C}(\mathbf{q}_2, \dot{\mathbf{q}}_2)\mathbf{s}_2 + \mathbf{K}_1\mathbf{s}_2 - \mathbf{K}_2\mathbf{s}_1(t - T_{12}) = \mathbf{0}
\end{aligned} \tag{62}$$

which can be shown to be semicontracting (asymptotically stable) using the following differential length similar to [29]:

$$V = \delta\mathbf{z}^T(\mathbf{V}^T[\mathbf{M}]\mathbf{V})\delta\mathbf{z} + V_{1,2}, \qquad \mathbf{z} = \mathbf{V}^T(\mathbf{s}_1^T, \mathbf{s}_2^T)^T \tag{63}$$

where

$$V_{1,2} = \int_{t-T_{12}}^{t} \delta\mathbf{v}_{12}^T\delta\mathbf{v}_{12}\,\mathrm{d}\epsilon + \int_{t-T_{21}}^{t} \delta\mathbf{v}_{21}^T\delta\mathbf{v}_{21}\,\mathrm{d}\epsilon \tag{64}$$

In conclusion, the formation flying spacecraft systems, individually contracting (exponentially converging) and interacting through time-delayed diffusionlike coupling, are asymptotically contracting regardless of the values of the time delays. This shows that the proposed control law and its closed-loop system in Eq. (28) possess some robustness properties with respect to time delays.

B. Effect of Bounded Disturbances

Equation (39), in the presence of the external disturbance torque τ_{ext}, can be written as

$$\begin{aligned}
&(\mathbf{V}^T[\mathbf{M}]\mathbf{V})\begin{pmatrix} [\mathbf{1}]^T\dot{\mathbf{x}} \\ \mathbf{V}_{\text{sync}}^T\dot{\mathbf{x}} \end{pmatrix} + (\mathbf{V}^T[\mathbf{C}]\mathbf{V} + [\mathbf{D}])\begin{pmatrix} [\mathbf{1}]^T\mathbf{x} \\ \mathbf{V}_{\text{sync}}^T\mathbf{x} \end{pmatrix} \\
&= \begin{pmatrix} [\mathbf{1}]^T \\ \mathbf{V}_{\text{sync}}^T \end{pmatrix}\begin{pmatrix} \tau_{\text{ext},\mathbf{1}} \\ \vdots \\ \tau_{\text{ext},\mathbf{p}} \end{pmatrix}
\end{aligned} \tag{65}$$

which indicates that the disturbance input for the synchronization is only the difference among each disturbance force/torque $\mathbf{V}_{\text{sync}}^T(\tau_{\text{ext},\mathbf{1}}^T, \ldots, \tau_{\text{ext},\mathbf{p}}^T)^T$. As a result, the disturbance torque that is invariant from spacecraft to spacecraft does not affect the synchronization of the relative attitude, which might be of more importance than the performance of trajectory following. For example, stellar interferometers need precise control of relative attitude and distance between spacecraft that carry telescopes.

Now we consider the bounded vanishing disturbance of the individual tracking dynamics. Because of exponential tracking convergence of the proposed scheme, the property of robustness to bounded deterministic disturbances can easily be determined. For example, consider the closed-loop system in Eq. (28), which is now subject to a vanishing perturbation [24] such that $\mathbf{d}(t, \mathbf{x} = \mathbf{0}) = \mathbf{0}$:

$$[\mathbf{M}]\dot{\mathbf{x}} + [\mathbf{C}]\mathbf{x} + [\mathbf{L}_{\mathbf{K}_1,-\mathbf{K}_2}^p]\mathbf{x} = \mathbf{d}(t, \mathbf{x}) \tag{66}$$

The perturbation term $\mathbf{d}(t, \mathbf{x})$ vanishes at the equilibrium manifold $\mathbf{x} = \mathbf{0}$. Let us further assume that it satisfies the linear growth bound such that

$$\|\mathbf{d}(t, \mathbf{x})\| \le \gamma\|\mathbf{x}\|, \quad \forall\ t\ > 0 \tag{67}$$

where γ is a positive constant.

The squared-length analysis yields

$$\begin{aligned}
\frac{\mathrm{d}}{\mathrm{d}t}(\delta\mathbf{x}^T[\mathbf{M}]\delta\mathbf{x}) &= 2\delta\mathbf{x}^T[\mathbf{M}]\delta\dot{\mathbf{x}} + \delta\mathbf{x}^T[\dot{\mathbf{M}}]\delta\mathbf{x} = 2\delta\mathbf{x}^T(-[\mathbf{C}]\delta\mathbf{x} \\
&\quad - [\mathbf{L}_{\mathbf{K}_1,-\mathbf{K}_2}^p]\delta\mathbf{x} + \delta\mathbf{d}(t, \mathbf{x})) + \delta\mathbf{x}^T[\dot{\mathbf{M}}]\delta\mathbf{x} \\
&\le -2\delta\mathbf{x}^T([\mathbf{L}_{\mathbf{K}_1,-\mathbf{K}_2}^p] - \gamma\mathbf{I})\delta\mathbf{x}
\end{aligned} \tag{68}$$

where we used the skew-symmetric property of $[\dot{\mathbf{M}}] - 2[\mathbf{C}]$.

Hence, the closed-loop system in Eq. (66) is contracting in the presence of the bounded disturbance if $[\mathbf{L}_{\mathbf{K}_1,-\mathbf{K}_2}^p] > \gamma\mathbf{I}$. As a result, the trajectory tracking gain (slower gain) also determines how robust the closed-loop system is with respect to a bounded disturbance.

For a nonvanishing perturbation such that

$$\|\mathbf{d}(t, \mathbf{x})\| \le \gamma\|\mathbf{x}\| + \Delta \tag{69}$$

where Δ is bounded, the comparison method [24] can straightforwardly be developed to derive a bound on the solution. Alternatively, we can follow the analysis of contraction with respect to a property of robustness [26,45].

We assume that $P_1(t)$ represents a desired system trajectory and $P_2(t)$ the actual system trajectory in a disturbed flow field given in Eq. (66). Also, consider the distance $R(t)$ between two trajectories $P_1(t)$ and $P_2(t)$ such that

$$R(t) = \int_{P_1}^{P_2} \|\delta\mathbf{z}\| = \int_{P_1}^{P_2} \|\mathbf{\Theta}(\mathbf{x})\delta\mathbf{x}\| \tag{70}$$

where $\mathbf{\Theta}(\mathbf{x})^T\mathbf{\Theta}(\mathbf{x}) = [\mathbf{M}]$ (see the Appendix).

Then, by combining the results from Eqs. (68) and (69) and [26], we can show that any trajectory converges exponentially to a ball of radius of R around the desired trajectory such that

$$R(t) \le \sup_{\mathbf{x},t}\|\mathbf{\Theta}(\mathbf{x})^{-T}\Delta\|/\lambda_{\max} \tag{71}$$

where the contraction rate $\lambda_{\max}$, in the context of contraction theory, is defined with respect to $\delta\mathbf{z} = \mathbf{\Theta}(\mathbf{x})\delta\mathbf{x}$ and is given by $[\mathbf{M}]^{-1}([\mathbf{L}_{\mathbf{K}_1,-\mathbf{K}_2}^p] - \gamma\mathbf{I})$ from Eq. (68). It should be emphasized that the exponential stability of the closed-loop system facilitates such a perturbation analysis, which showcases another benefit of contraction analysis. In contrast, the proof of robustness with asymptotic convergence is more involved [24].

VI. Extensions and Examples

Let us examine the effectiveness of the proposed control law in a few examples.

A. Synchronization with Partial Degrees-of-Freedom Coupling

In this section, we consider multiple spacecraft with partially coupled variables. For instance, we can assume that only the first and third MRP variables (q_1 and q_3) are coupled in a two-spacecraft system such that

$$\begin{aligned}
\tau_1 &= \mathbf{M}(\mathbf{q}_1)\ddot{\mathbf{q}}_{1r} + \mathbf{C}(\mathbf{q}_1, \dot{\mathbf{q}}_1)\dot{\mathbf{q}}_{1r} + \mathbf{g}(\mathbf{q}_1) - \mathbf{K}_1\mathbf{s}_1 \\
&\quad + \mathbf{K}_2\begin{pmatrix} \dot{\tilde{q}}_1 & 0 & \dot{\tilde{q}}_3 \end{pmatrix}_{\mathbf{q}_2}^T + \mathbf{K}_2\mathbf{\Lambda}\begin{pmatrix} \tilde{q}_1 & 0 & \tilde{q}_3 \end{pmatrix}_{\mathbf{q}_2}^T \\
\tau_2 &= \mathbf{M}(\mathbf{q}_2)\ddot{\mathbf{q}}_{2r} + \mathbf{C}(\mathbf{q}_2, \dot{\mathbf{q}}_2)\dot{\mathbf{q}}_{2r} + \mathbf{g}(\mathbf{q}_2) - \mathbf{K}_1\mathbf{s}_2 \\
&\quad + \mathbf{K}_2\begin{pmatrix} \dot{\tilde{q}}_1 & 0 & \dot{\tilde{q}}_3 \end{pmatrix}_{\mathbf{q}_1}^T + \mathbf{K}_2\mathbf{\Lambda}\begin{pmatrix} \tilde{q}_1 & 0 & \tilde{q}_3 \end{pmatrix}_{\mathbf{q}_1}^T
\end{aligned} \tag{72}$$

Nonetheless, Theorems III.1 and III.2 are true with diagonal matrices $\mathbf{K}_1$, $\mathbf{K}_2$, and $\mathbf{\Lambda}$, which can be verified by writing the closed-loop system as

$$\mathbf{M}(\mathbf{q}_1)\dot{\mathbf{s}}_1 + \mathbf{C}(\mathbf{q}_1, \dot{\mathbf{q}}_1)\mathbf{s}_1 + (\mathbf{K}_1 + \mathbf{K}_2\mathbf{P})\mathbf{s}_1 = \mathbf{u}(t)$$
$$\mathbf{M}(\mathbf{q}_2)\dot{\mathbf{s}}_2 + \mathbf{C}(\mathbf{q}_2, \dot{\mathbf{q}}_2)\mathbf{s}_2 + (\mathbf{K}_1 + \mathbf{K}_2\mathbf{P})\mathbf{s}_2 = \mathbf{u}(t) \qquad (73)$$
$$\mathbf{u}(t) = \mathbf{K}_2\mathbf{P}(\mathbf{s}_1 + \mathbf{s}_2)$$

where $\mathbf{P} = \mathrm{diag}(1, 0, 1)$.

We can prove that Theorems III.1 and III.2 still hold by showing that $\mathbf{K}_1 + \mathbf{K}_2\mathbf{P}$ and $\mathbf{K}_1 - \mathbf{K}_2\mathbf{P}$ are still uniformly positive definite, enabling exponential synchronization and exponential convergence to the desired trajectory, respectively. Hence, we did not break any assumptions in the proof of Theorem III.2.

B. Attitude Synchronization of Two Spacecraft

The proposed control law in Eq. (23) is simulated for two identical spacecraft, as shown in Fig. 6a. The spacecraft inertial matrix is

$$\mathbf{J}_{s/c} = \begin{bmatrix} 150 & 0 & -100 \\ 0 & 270 & 0 \\ -100 & 0 & 300 \end{bmatrix} [\mathrm{kg} \cdot \mathrm{m}^2] \qquad (74)$$

The control gains are defined as $\mathbf{K}_1 = 300\mathbf{I}$, $\mathbf{K}_2 = 100\mathbf{I}$, and $\mathbf{\Lambda} = 20\mathbf{I}$. The reference trajectories are defined as $\mathbf{q}_{1d} = 0.3\sin(2\pi(0.01)t)$, $\mathbf{q}_{2d} = 0.2\sin(2\pi(0.02)t + \pi/6)$, and $\mathbf{q}_{3d} = 0$. The first spacecraft is initially at $(0.05, -0.1, 0)^T$ rad, with zero angular rates, whereas all the initial conditions for the second spacecraft are zero.

The synchronization gain of $\mathbf{s}_1$ and $\mathbf{s}_2$ corresponds to $\mathbf{K}_1 + \mathbf{K}_2 = 400\mathbf{I}$, which is larger than the tracking convergence gain $\mathbf{K}_1 - \mathbf{K}_2 = 200\mathbf{I}$. As a result, we can see in Fig. 6 that the first and second spacecraft exponentially synchronize first. Then, they exponentially converge together to the desired trajectory.

To compare the effectiveness of the exponential tracking, a simple proportional and derivative (PD) diffusive coupling, introduced in [4,22], is simulated for the comparison purpose, as shown in Fig. 6b. The control law for two spacecraft can be given as

$$\tau_1 = -\mathbf{K}_1(\dot{\mathbf{q}}_1 + \mathbf{\Lambda}\tilde{\mathbf{q}}_1) + \mathbf{K}_2(\dot{\mathbf{q}}_2 + \mathbf{\Lambda}\tilde{\mathbf{q}}_2)$$
$$\tau_2 = -\mathbf{K}_1(\dot{\mathbf{q}}_2 + \mathbf{\Lambda}\tilde{\mathbf{q}}_2) + \mathbf{K}_2(\dot{\mathbf{q}}_1 + \mathbf{\Lambda}\tilde{\mathbf{q}}_1) \qquad (75)$$

whose global asymptotic stability with respect to a constant reference input is proven in [4,22]. For a fair comparison, we selected the PD gains in Eq. (75) as $\mathbf{K}_1 = 1000$, $\mathbf{K}_2 = 300$, and $\mathbf{\Lambda} = 0.3$ such that the level of control efforts is comparable to that of the nonlinear control approach in Eq. (23). As shown in Fig. 6b, the PD coupling control law is not effective in following a time-varying trajectory. This is because simple linear control cannot be expected to handle the dynamic demands of efficiently following time-varying trajectories. In contrast, the proposed nonlinear approach shown in Fig. 6a exponentially synchronizes the attitude states, while the tracking errors tend exponentially to zero. Specifically, achieving exponential convergence ensures more effective tracking performance than asymptotic convergence by linear PD control. The proposed nonlinear control law with the given initial condition and control gains introduces a large control effort initially. However, the results do not change, even if the torque actuators saturate at ± 6 N · m.

C. Four Spacecraft Example

To illustrate the effectiveness of the proposed approach for a larger formation, a result of simulation for four nonidentical spacecraft is presented in Fig. 7. The spacecraft inertia matrices are

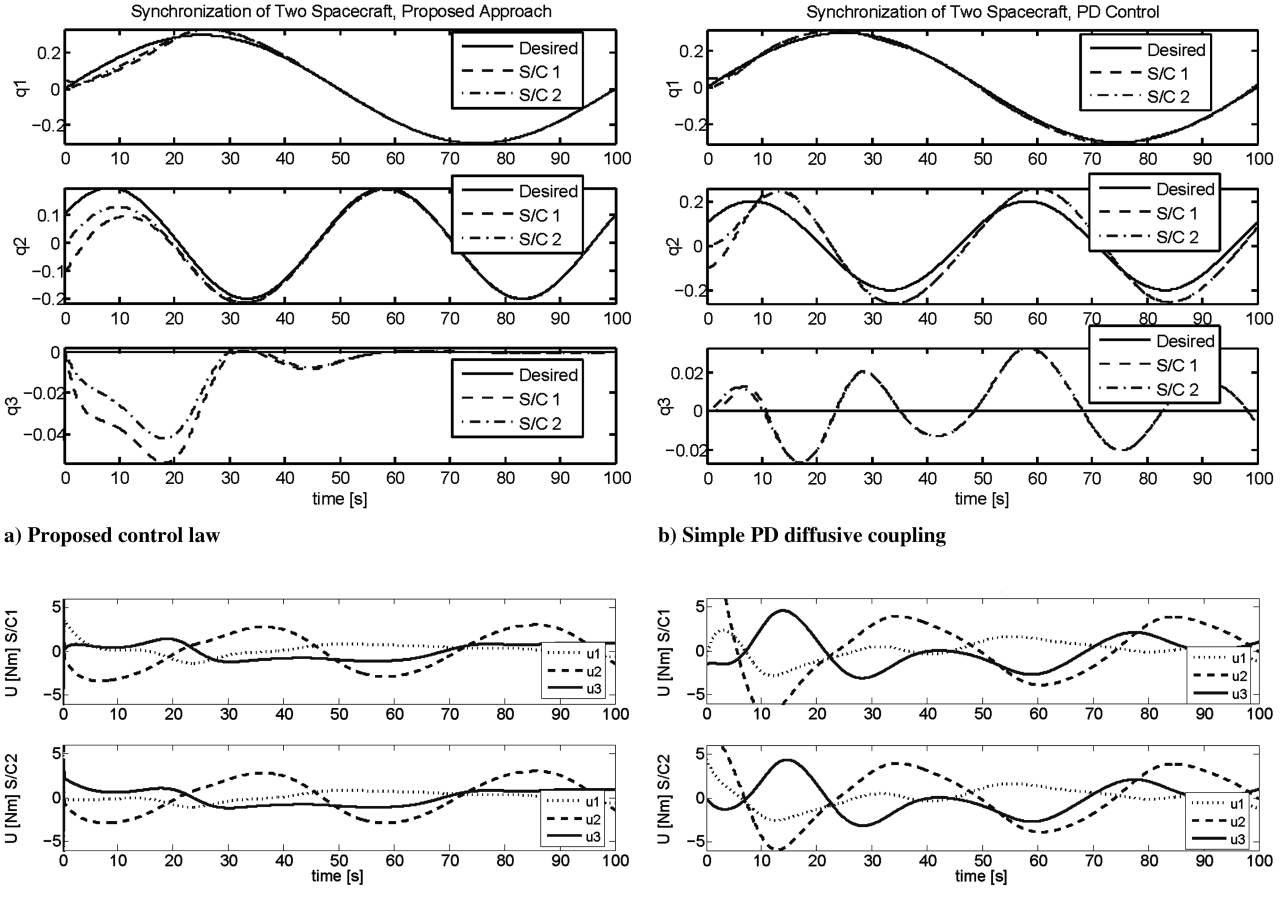

a) Proposed control law

b) Simple PD diffusive coupling

c) Control effort: proposed control

d) Control effort: PD control

Fig. 6 Synchronization of the attitude dynamics of two identical spacecraft.

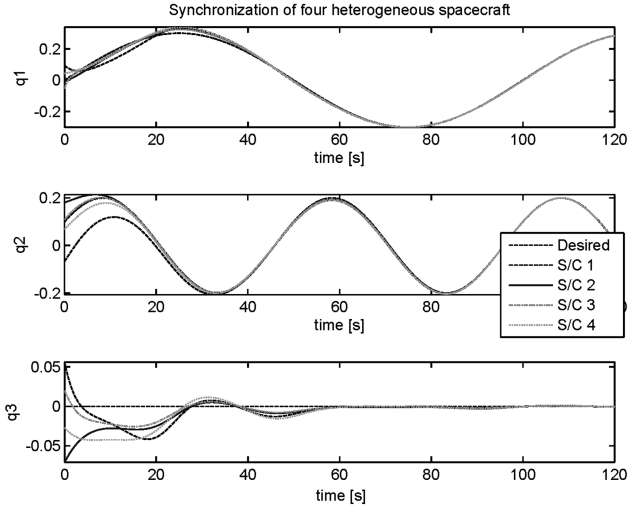

a) States q_1, q_2, q_3

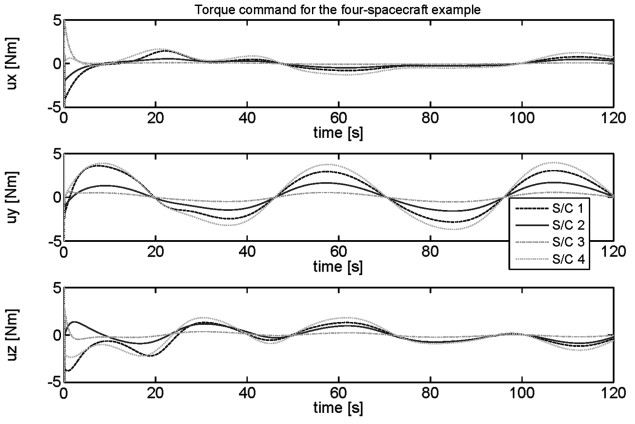

b) Commanded torque

Fig. 7 Synchronization of four heterogeneous spacecraft.

$$\begin{bmatrix} 150 & 0 & -100 \\ 0 & 270 & 0 \\ -100 & 0 & 300 \end{bmatrix}, \quad \begin{bmatrix} 100 & 0 & -50 \\ 0 & 150 & 0 \\ -50 & 0 & 250 \end{bmatrix}$$
$$\begin{bmatrix} 20 & 0 & -5 \\ 0 & 50 & 0 \\ -5 & 0 & 65 \end{bmatrix}, \quad \begin{bmatrix} 250 & 0 & -150 \\ 0 & 350 & 0 \\ -150 & 0 & 400 \end{bmatrix} \text{ in } [\text{kg} \cdot \text{m}^2] \tag{76}$$

respectively. The desired trajectories are the same as in the previous section, and the control gains remain the same as well, such that the tracking convergence gain is $\mathbf{K}_1 - 2\mathbf{K}_2 = 100\mathbf{I} > 0$. Figure 7 shows that the four spacecraft synchronize themselves while following the desired trajectory together.

D. Position and Attitude Synchronization of Two Spacecraft Under J_2 Effect

A full 6 DOF simulation of a two identical satellite formation using the proposed phase synchronization control law (45) and with the attitude tracking Eq. (2) was prepared. Full nonlinear attitude and translational dynamics including the J2 effect were simulated for each satellite in the formation. The mass of each satellite is assumed to be 500 kg. The spacecraft inertia matrix is given by Eq. (74). The attitude control gains were defined as $\mathbf{K}_1 = 30\mathbf{I}$, $\mathbf{K}_2 = 20\mathbf{I}$, and $\mathbf{\Lambda} = 20\mathbf{I}$. The attitude reference trajectories were defined to be $q_{1d} = 0.3\sin(2\pi \times 0.001t)$, $q_{2d} = 0.2\sin(2\pi \times 0.002t + \pi/6)$, and $q_{3d} = 0$, which are similar (but at a lower frequency) to the previous example.

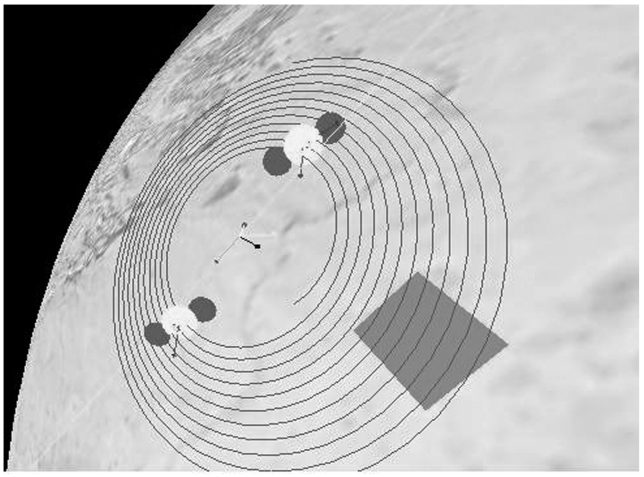

Fig. 8 Three-dimensional simulation of the phase synchronization on a spiral trajectory.

For the translational control the gains were defined to be the same for both the satellites as $k_1 = 10$, $k_2 = 5$, and $\lambda = 2$. The desired trajectory for the formation was defined so that the satellites would follow a spiral trajectory such that both satellites maintain a phase angle of 180 deg. The desired spiral trajectory was defined as $\mathbf{r}_d = [a(t)\sin\omega t, 0, a(t)\cos\omega t]^T$ from Eq. (48), where $a(t) = 5 + 0.0001t$ and $\omega = 2\pi/500$ (see the actual plot of this spiral trajectory generated from the actual simulation in Fig. 8). The formation was placed in a polar circular orbit at an altitude of 500 km and it was subject to J2 perturbations in the nonlinear model. Figure 9 shows the robust synchronization performance in the presence of nonidentical disturbance such as the differential J2 effect. It should be noted that this scheme requires information from only the adjacent spacecraft; thus this scheme is suitable for implementing a distributed control architecture.

VII. Conclusions

We have introduced the new unified synchronization framework that integrates both the exponential tracking of a demanding time-varying trajectory and the synchronization of spacecraft motions either through local coupling feedback or a relative sensing metrology system. The new decentralized control laws, developed by using the Lagrangian formulations of the translational dynamics and attitude dynamics of spacecraft, enable coupled rotational maneuvers and phase synchronization of the attitude and position, thereby facilitating a further analysis on stability, adaptation, and robustness. To rigorously address the three main areas of research for the realization of future spacecraft formation flying missions, we have focused on the three research areas: 1) the exact nonlinear stability conditions of multiple spacecraft dynamics, 2) the reduced information networks through partial-state couplings and local interactions, and 3) the properties of robustness with respect to uncertain models and time delays of the communication. In particular, in contrast with prior work which used simple single or double integrator models, the proposed method is applicable to highly nonlinear systems with nonlinearly coupled inertia matrices such as the attitude dynamics of spacecraft. A main contribution of this paper is to provide exact proofs of nonlinear stability and convergence under a variety of conditions, based on nonlinear contraction theory, a comparatively recent analysis tool. Contraction analysis, overcoming a local result of Lyapunov's indirect method, yields global results based on differential stability analysis. The benefit of constructing multiple time scales of the closed-loop system is that exponential synchronization, with a convergence rate faster than that of the trajectory tracking, enables reduction of multiple dynamics into a simpler synchronized form, thereby simplifying the additional stability analysis. The proposed bidirectional coupling has also been generalized to permit partial-state coupling, thereby further reducing communication requirements. We illustrated the effective-

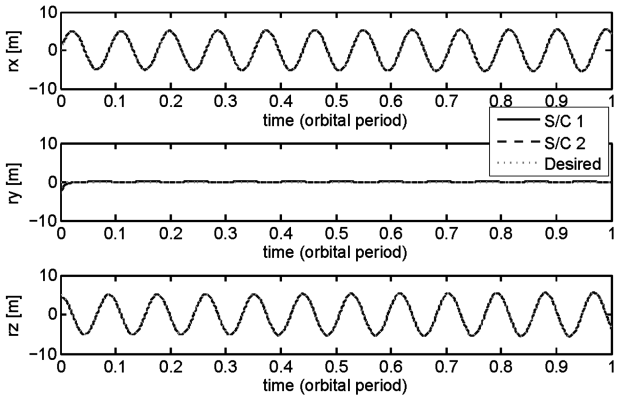

a) Results of the simulation for two spacecraft phase synchronization

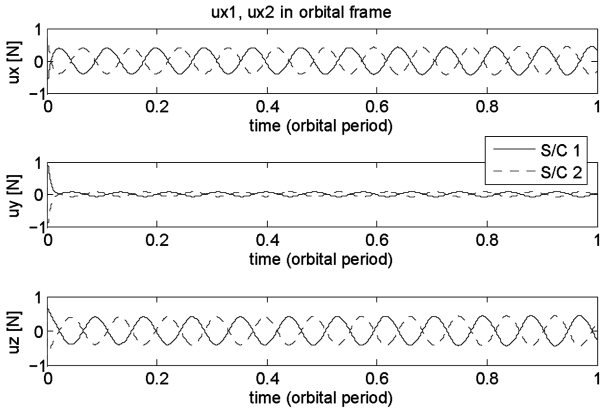

b) Control forces

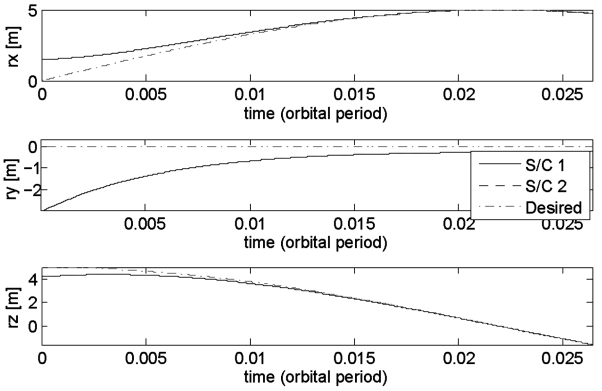

c) Initial synchronization of the formation with the desired trajectory

Fig. 9 Simulation of the proposed control law for the combined translational and rotational dynamics.

ness of the proposed approach by comparing with the simple PD coupling control law, and simulating the combined rotational and translational maneuvers in the presence of variation in the second-degree zonal harmonic J2 of the Earth's gravitational potential.

Appendix: Contraction Theory

We exploit the partial contraction theory [28] to prove the stability of coupled nonlinear dynamics. Lyapunov's linearization method indicates that the local stability of the nonlinear system can be analyzed using its differential approximation. What is new in contraction theory is that a differential stability analysis can be made exact, thereby yielding global results on the nonlinear system. A brief review of the results from [26–28] is presented in this section. Readers are referred to these references for detailed descriptions and proofs on the following theorems. Note that contraction theory is a generalization of the classical Krasovskii's theorem [23].

Consider a smooth nonlinear system

$$\dot{\mathbf{x}}(t) = \mathbf{f}(\mathbf{x}(t), \mathbf{u}(\mathbf{x}, t), t) \tag{A1}$$

where $\mathbf{x}(t) \in \mathbb{R}^n$, and $\mathbf{f}$: $\mathbb{R}^n \times \mathbb{R}^m \times \mathbb{R}_+ \to \mathbb{R}^n$. A virtual displacement $\delta\mathbf{x}$ is defined as an infinitesimal displacement at a fixed time—a common supposition in the calculus of variations.

Theorem VII.1: For the system in Eq. A1, if there exists a uniformly positive-definite metric,

$$\mathbf{M}(\mathbf{x}, t) = \mathbf{\Theta}(\mathbf{x}, t)^T \mathbf{\Theta}(\mathbf{x}, t) \tag{A2}$$

where $\mathbf{\Theta}$ is some smooth coordinate transformation of the virtual displacement, $\delta\mathbf{z} = \mathbf{\Theta}\delta\mathbf{x}$, such that the associated generalized Jacobian $\mathbf{F}$ is uniformly negative definite, that is, $\exists\lambda > 0$ such that

$$\mathbf{F} = \left(\dot{\mathbf{\Theta}}(\mathbf{x}, t) + \mathbf{\Theta}(\mathbf{x}, t)\frac{\partial \mathbf{f}}{\partial \mathbf{x}}\right)\mathbf{\Theta}(\mathbf{x}, t)^{-1} \leq -\lambda\mathbf{I} \tag{A3}$$

then all system trajectories converge globally to a single trajectory exponentially fast regardless of the initial conditions, with a global exponential convergence rate of the largest eigenvalues of the symmetric part of $\mathbf{F}$.

Such a system is said to be contracting. The proof is given in [26]. Equivalently, the system is contracting if $\exists\lambda > 0$ such that

$$\dot{\mathbf{M}} + \left(\frac{\partial \mathbf{f}}{\partial \mathbf{x}}\right)^T \mathbf{M} + \mathbf{M}\frac{\partial \mathbf{f}}{\partial \mathbf{x}} \leq -2\lambda\mathbf{M} \tag{A4}$$

It can also be shown that for a contracting autonomous system of the form $\dot{\mathbf{x}} = \mathbf{f}(\mathbf{x}, \mathbf{u}(\mathbf{x}))$, all trajectories converge to an equilibrium point exponentially fast. In essence, contraction analysis implies that stability of nonlinear systems can be analyzed more simply by checking the negative definiteness of a proper matrix, rather than finding some implicit motion integral as in the Lyapunov theory.

The following theorems are used to derive stability and synchronization of the coupled dynamics systems.

Theorem VII.2: Hierarchical Combination [27,28]. Consider two contracting systems, of possibly different dimensions and metrics, and connect them in series, leading to smooth virtual dynamics of the form

$$\frac{d}{dt}\begin{pmatrix}\delta\mathbf{z}_1 \\ \delta\mathbf{z}_2\end{pmatrix} = \begin{pmatrix}\mathbf{F}_{11} & \mathbf{0} \\ \mathbf{F}_{21} & \mathbf{F}_{22}\end{pmatrix}\begin{pmatrix}\delta\mathbf{z}_1 \\ \delta\mathbf{z}_2\end{pmatrix}$$

Then the combined system is contracting if $\mathbf{F}_{21}$ is bounded.

Theorem VII.3: Partial Contraction [28]. Consider a nonlinear system of the form $\dot{\mathbf{x}} = \mathbf{f}(\mathbf{x}, \mathbf{x}, t)$ and assume that the auxiliary system $\dot{\mathbf{y}} = \mathbf{f}(\mathbf{y}, \mathbf{x}, t)$ is contracting with respect to $\mathbf{y}$. If a particular solution of the auxiliary $\mathbf{y}$ system verifies a specific smooth property, then all trajectories of the original x system verify this property exponentially. The original system is said to be partially contracting.

Theorem VII.4: Synchronization [28]. Consider two coupled systems. If the dynamics equations verify

$$\dot{\mathbf{x}}_1 - \mathbf{f}(\mathbf{x}_1, t) = \dot{\mathbf{x}}_2 - \mathbf{f}(\mathbf{x}_2, t)$$

where the function $\mathbf{f}(\mathbf{x}, t)$ is contracting in an input-independent metric, then $\mathbf{x}_1$ and $\mathbf{x}_2$ will converge to each other exponentially, regardless of the initial conditions. Mathematically, stable concurrent synchronization corresponds to convergence to a flow-invariant linear subspace of the global state space [45].

Acknowledgments

This work has benefitted from stimulating discussions with David W. Miller at Massachusetts Institute of Technology (MIT), Bong Wie at Iowa State University, and Jesse Leitner at the NASA Goddard Space Flight Center. S.-J. Chung thanks Insu Chang for carefully reviewing the paper. The authors would like to acknowledge the constructive feedback from the Associate Editor (Hanspeter Schaub) and anonymous reviewers.

References

[1] Leitner, J., Carpenter, J. R., Naasz, B. J., Ahmed, A., Hadaegh, F. Y., and Scharf, D. P., "A Concept for In-Space, System-Level Validation of Spacecraft Precision Formation Flying," AIAA Paper 2007-6541, Aug. 2007.

[2] Chung, S.-J., Slotine, J.-J. E., and Miller, D. W., "Nonlinear Model Reduction and Decentralized Control of Tethered Formation Flight," *Journal of Guidance, Control, and Dynamics*, Vol. 30, No. 2, 2007, pp. 390–400. doi:10.2514/1.21492

[3] Ahsun, U., "Dynamics and Control of Electromagnetic Satellite Formations," Ph.D. Thesis, Department of Aeronautics and Astronautics, Massachusetts Institute of Technology, Cambridge, MA, 2007, http://dspace.mit.edu.

[4] Chung, S.-J., "Nonlinear Control and Synchronization of Multiple Lagrangian Systems with Application to Tethered Formation Flight Spacecraft," Sc.D. Thesis, Department of Aeronautics and Astronautics, Massachusetts Institute of Technology, Cambridge, MA, 2007, http://dspace.mit.edu.

[5] Chung, S.-J., Miller, D. W., and de Weck, O. L., "ARGOS Testbed: Study of Multidisciplinary Challenges of Future Spaceborne Interferometric Arrays," *Optical Engineering (Bellingham, Washington)*, Vol. 43, No. 9, Sept. 2004, pp. 2156–2167. doi:10.1117/1.1779232

[6] Scharf, D. P., Hadaegh, F. Y., and Ploen, S. R., "A Survey of Spacecraft Formation Flying Guidance and Control (Part 1): Guidance," *Proceedings of the American Control Conference*, IEEE, Piscataway, NJ, 4–6 June 2003, pp. 1733–1739.

[7] Scharf, D. P., Hadaegh, F. Y., and Ploen, S. R., "A Survey of Spacecraft Formation Flying Guidance and Control (Part 2): Control," *Proceedings of the American Control Conference*, IEEE, Piscataway, NJ, 4–6 June 2003, pp. 2976–2985.

[8] Olfati-Saber, R., and Murray, R. M., "Consensus Problems in Networks of Agents with Switching Topology and Time-Delays," *IEEE Transactions on Automatic Control*, Vol. 49, No. 9, Sept. 2004, pp. 1520–1533. doi:10.1109/TAC.2004.834113

[9] Olfati-Saber, R., "Flocking for Multi-Agent Dynamic Systems: Algorithms and Theory," *IEEE Transactions on Automatic Control*, Vol. 51, No. 3, 2006, pp. 401–420. doi:10.1109/TAC.2005.864190

[10] Jadbabaie, A., Lin, J., and Morse, A. S., "Coordination of Groups of Mobile Autonomous Agents Using Nearest Neighbor Rules," *IEEE Transactions on Automatic Control*, Vol. 48, No. 6, June 2003, pp. 988–1001. doi:10.1109/TAC.2003.812781

[11] Mesbahi, M., and Hadaegh, F. Y., "Formation Flying of Multiple Spacecraft via Graphs, Matrix Inequalities, and Switching," *Journal of Guidance, Control, and Dynamics*, Vol. 24, No. 2, 2001, pp. 369–377. doi:10.2514/2.4721

[12] Wang, P. K. C., and Hadaegh, F. Y., "Coordination and Control of Multiple Microspacecraft Moving in Formation," *Journal of the Astronautical Sciences*, Vol. 44, No. 3, July–Sept. 1996, pp. 315–355.

[13] Wang, P. K. C., Hadaegh, F. Y., and Lau, K., "Synchronized Formation Rotation and Attitude Control of Multiple Free-Flying Spacecraft," *Journal of Guidance, Control, and Dynamics*, Vol. 22, No. 1, 1999, pp. 28–35. doi:10.2514/2.4367

[14] Pan, H., and Kapila, V., "Adaptive Nonlinear Control for Spacecraft Formation Flying with Coupled Translational and Attitude Dynamics," *Proceedings of the 40th IEEE Conference on Decision and Control*, IEEE, Piscataway, NJ, Vol. 3, Dec. 2001, pp. 2057–2062.

[15] Lawton, J., and Beard, R. W., "Synchronized Multiple Spacecraft Rotations," *Automatica*, Vol. 38, No. 8, 2002, pp. 1359–1364. doi:10.1016/S0005-1098(02)00025-0

[16] Beard, R. W., Lawton, J., and Hadaegh, F. Y., "A Coordination Architecture for Spacecraft Formation Control," *IEEE Transactions on Control Systems Technology*, Vol. 9, No. 6, Nov. 2001, pp. 777–790. doi:10.1109/87.960341

[17] Ren, W., and Beard, R. W., "Decentralized Scheme for Spacecraft Formation Flying via the Virtual Structure Approach," *Journal of Guidance, Control, and Dynamics*, Vol. 27, No. 1, Jan.–Feb. 2004, pp. 73–82. doi:10.2514/1.9287

[18] VanDyke, M. C., and Hall, C. D., "Decentralized Coordinated Attitude Control Within a Formation of Spacecraft," *Journal of Guidance, Control, and Dynamics*, Vol. 29, No. 5, Sept.–Oct. 2006, pp. 1101–1109. doi:10.2514/1.17857

[19] Ren, W., "Formation Keeping and Attitude Alignment for Multiple Spacecraft Through Local Interactions," *Journal of Guidance, Control, and Dynamics*, Vol. 30, No. 2, March–April 2007, pp. 633–638. doi:10.2514/1.25629

[20] Ren, W., "Distributed Attitude Alignment in Spacecraft Formation Flying," *International Journal of Adaptive Control and Signal Processing*, Vol. 21, Nos. 2–3, March–April 2007, pp. 95–113. doi:10.1002/acs.916

[21] Paley, D. A., Leonard, N. E., Sepulchre, R., Grunbaum, D., and Parrish, J. K., "Oscillator Models and Collective Motion: Spatial Patterns in the Dynamics of Engineered and Biological Networks," *IEEE Control Systems Magazine*, Vol. 27, No. 4, Aug. 2007, pp. 89–105. doi:10.1109/MCS.2007.384123

[22] Chung, S.-J., and Slotine, J.-J. E., "Cooperative Robot Control and Concurrent Synchronization of Lagrangian Systems," *IEEE Transactions on Robotics* (to be published).

[23] Slotine, J.-J. E., and Li, W., *Applied Nonlinear Control*, Prentice–Hall, Upper Saddle River, NJ, 1991, pp. 41–154.

[24] Khalil, H. K., *Nonlinear Systems*, 3rd ed., Prentice–Hall, Upper Saddle River, NJ, 2002, pp. 339–372.

[25] Wie, B., *Space Vehicle Dynamics and Control*, AIAA, Reston, VA, 1998, pp. 435–445.

[26] Lohmiller, W., and Slotine, J. J. E., "On Contraction Analysis for Nonlinear Systems," *Automatica*, Vol. 34, No. 6, 1998, pp. 683–696. doi:10.1016/S0005-1098(98)00019-3

[27] Slotine, J.-J. E., "Modular Stability Tools for Distributed Computation and Control," *International Journal of Adaptive Control and Signal Processing*, Vol. 17, No. 6, 2003, pp. 397–416. doi:10.1002/acs.754

[28] Wang, W., and Slotine, J. J. E., "On Partial Contraction Analysis for Coupled Nonlinear Oscillators," *Biological Cybernetics*, Vol. 92, No. 1, 2005, pp. 38–53. doi:10.1007/s00422-004-0527-x

[29] Wang, W., and Slotine, J.-J. E., "Contraction Analysis of Time-Delayed Communications Using Simplified Wave Variables," *IEEE Transactions on Automatic Control*, Vol. 51, No. 4, 2006, pp. 712–717. doi:10.1109/TAC.2006.872761

[30] Lee, D., and Li, P. Y., "Formation and Maneuver Control of Multiple Spacecraft," *Proceedings of the 2003 American Control Conference*, IEEE, Piscataway, NJ, Vol. 1, June 2003, pp. 278–283.

[31] Carpenter, J. R., "Decentralized Control of Satellite Formations," *International Journal of Robust and Nonlinear Control*, Vol. 12, Nos. 2–3, 2002, pp. 141–161. doi:10.1002/rnc.680

[32] Vadali, S. R., Vaddi, S. S., Naik, K., and Alfriend, K. T., "Control of Satellite Formations," AIAA Paper 2001-4028, 6–9 Aug. 2001.

[33] Kasdin, N. J., Gurfil, P., and Kolemen, E., "Canonical Modeling of Relative Spacecraft Motion via Epicyclic Orbital Elements," *Celestial Mechanics and Dynamical Astronomy*, Vol. 92, No. 4, 2005, pp. 337–370. doi:10.1007/s10569-004-6441-7

[34] Schaub, H., Vadali, S. R., Junkins, J. L., and Alfriend, K. T., "Spacecraft Formation Flying Control Using Mean Orbit Elements," *Journal of the Astronautical Sciences*, Vol. 48, No. 1, Jan.–March 2000, pp. 69–87.

[35] Breger, L., and How, J. P., "Gauss's Variational Equation-Based Dynamics and Control for Formation Flying Spacecraft," *Journal of*

Guidance, Control, and Dynamics, Vol. 30, No. 2, 2007, pp. 437–448. doi:10.2514/1.22649

[36] Yeh, H.-H., Nelson, E., and Sparks, A., "Nonlinear Tracking Control for Satellite Formations," *Journal of Guidance, Control, and Dynamics*, Vol. 25, No. 2, March–April 2002, pp. 376–386. doi:10.2514/2.4892

[37] Slotine, J.-J. E. and Benedetto, M. D. D., "Hamiltonian Adaptive Control of Spacecraft," *IEEE Transactions on Automatic Control*, Vol. 35, No. 7, July 1990, pp. 848–852. doi:10.1109/9.57028

[38] Yoon, H., and Tsiotras, P., "Spacecraft Adaptive Attitude and Power Tracking with Variable Speed Control Moment Gyroscopes," *Journal of Guidance, Control, and Dynamics*, Vol. 25, No. 6, Nov.–Dec. 2002, pp. 1081–1090. doi:10.2514/2.4987.

[39] Shuster, M. D., "A Survey of Attitude Representations," *Journal of the Astronautical Sciences*, Vol. 41, No. 4, 1993, pp. 439–517.

[40] Schaub, H., and Junkins, J. L., "Stereographic Orientation Parameters for Attitude Dynamics: A Generalization of the Rodrigues Parameters," *Journal of the Astronautical Sciences*, Vol. 44, No. 1, Jan.–March 1993, pp. 1–19.

[41] Ploen, S. R., Hadaegh, F. Y., and Scharf, D. P., "Ridgid Body Equations of Motion for Modeling and Control of Spacecraft Formations—Part 1: Absolute Equations of Motion," *Proceedings of the 2004 American Control Conference*, IEEE, Piscataway, NJ, 2004, pp. 3646–3653.

[42] Lim, R. S., and Miller, D. W., "Staged Attitude-Metrology Pointing Control and Parametric Integrated Modeling for Space-Based Optical Systems," M.Sc. Thesis, Space Systems Laboratory Rept. No. 3-06, Department of Aeronautics and Astronautics, Massachusetts Institute of Technology, Cambridge, MA, 2006, http://dspace.mit.edu.

[43] Kim, S.-G., Crassidis, J. L., Cheng, Y., Fosbury, A. M., and Junkins, J. L., "Kalman Filtering for Relative Spacecraft Attitude and Position Estimation," *Journal of Guidance, Control, and Dynamics*, Vol. 30, No. 1, Jan.–Feb. 2007, pp. 133–143. doi:10.2514/1.22377

[44] Smith, R. S., and Hadaegh, F. Y., "Control of Deep-Space Formation-Flying Spacecraft: Relative Sensing and Switched Information," *Journal of Guidance, Control, and Dynamics*, Vol. 28, No. 1, Jan.–Feb. 2005, pp. 106–114. doi:10.2514/1.6165

[45] Pham, Q.-C., and Slotine, J.-J. E., "Stable Concurrent Synchronization in Dynamic System Networks," *Neural Networks*, Vol. 20, No. 1, 2007, pp. 62–77. doi:10.1016/j.neunet.2006.07.008

[46] Strang, G., *Introduction to Applied Mathematics*, Wellesley-Cambridge Press, Wellesley, MA, 1986.